

2014

Autologous Adipose Derived Adult Multipotent Stromal Cells Alter the Porcine Systemic Immune and Bone Biomarkers Response to Cancellous Bone Xenografts

Jonathan Francis Bova
Louisiana State University and Agricultural and Mechanical College

Follow this and additional works at: https://digitalcommons.lsu.edu/gradschool_theses



Part of the [Veterinary Pathology and Pathobiology Commons](#)

Recommended Citation

Bova, Jonathan Francis, "Autologous Adipose Derived Adult Multipotent Stromal Cells Alter the Porcine Systemic Immune and Bone Biomarkers Response to Cancellous Bone Xenografts" (2014). *LSU Master's Theses*. 1065.

https://digitalcommons.lsu.edu/gradschool_theses/1065

This Thesis is brought to you for free and open access by the Graduate School at LSU Digital Commons. It has been accepted for inclusion in LSU Master's Theses by an authorized graduate school editor of LSU Digital Commons. For more information, please contact gradetd@lsu.edu.

AUTOLOGOUS ADIPOSE DERIVED ADULT MULTIPOTENT STROMAL
CELLS ALTER THE PORCINE SYSTEMIC IMMUNE AND BONE
BIOMARKER RESPONSE TO CANCELLOUS BONE XENOGRAFTS

A Thesis

Submitted to the Graduate Faculty of the
Louisiana State University and
Agricultural and Mechanical College
in partial fulfillment of the
requirements for the degree of
Master of Science

in

The Department of Pathobiological Sciences

by

Jonathan F. Bova, DVM
B.S., University of Arkansas, 2006
DVM, Louisiana State University, 2011
December 2014

ACKNOWLEDGEMENTS

There are many people without whom this thesis would not have been possible. I am very grateful for my major professor, Dr. Mandi J. Lopez, who allowed me to work with her lab and gave me the tools necessary to perform my research. Her guidance was essential in my completion of this research. I would also like to thank all the member of the Laboratory of Equine and Comparative Orthopedic Research (LECOR) for their assistance in all aspects of this study. Their assistance in data collection and pig handling made the process much more efficient.

I am also grateful to the other members of my graduate committee; Dr. Rhett W. Stout, Dr. Anderson F. da Cunha, and Dr. Philip H. Elzer. Dr. Stout was a great mentor both in research and in my residency training. Dr. da Cunha was a great resource for the anesthesia and pain assessment portions of the research. Dr. Elzer played an important role in helping me to understand and describe the immunology aspect of the research.

Finally, I am especially appreciative of my wife, Yvette, and all the members of my family. They are the ones who supported me throughout this entire process and helped to keep me on course. I know that without their love and support I would achieve nothing.

TABLE OF CONTENTS

ACKNOWLEDGEMENTS	ii
ABSTRACT	v
CHAPTER 1: LITERATURE REVIEW	1
1.1 Adipose Derived Multipotent Stromal Cell Introduction	1
1.1.1 Multipotent Stromal Cell Definition and Nomenclature	1
1.2 Therapeutic Effects of Adipose Derived Multipotent Stromal Cells	2
1.2.1 Differentiation Capabilities Of Adipose Derived Multipotent Stromal Cells	2
1.2.2 Trophic Effects Of Adipose Derived Multipotent Stromal Cells	2
1.2.3 Immune Modulatory Effects Of Adipose Derived Multipotent Stromal Cells	3
1.3 Bone Remodeling and Grafting	4
1.3.1 Physiology And Biology Of Bone Remodeling	4
1.3.2 Bone Graft Models And Nomenclature	5
1.3.3 Bone Graft Healing	6
1.4 Serum Biomarkers Of Bone Remodeling	7
1.4.1 Serum Biomarkers	7
CHAPTER 2: THE EFFECT OF A BUPIVACAINE MANDIBULAR NERVE BLOCK ON INTRAOPERATIVE CHANGES IN BLOOD PRESSURE AND HEART RATE AND THE NEED FOR POST-OPERATIVE ANALGESICS IN A YUCATAN MINIATURE SWINE MANDIBULAR CONDYLECTOMY MODEL: A PILOT STUDY	9
2.1 Introduction	9
2.2 Materials And Methods	10
2.2.1 Animals And Husbandry	10
2.2.2 Experimental Groups	11
2.2.3 Nerve Block and Rescue Analgesia	12
2.2.4 Surgical Procedure	13
2.2.5 Postoperative Pain Assessment	15
2.2.6 Statistics	16
2.3 Results	16
2.3.1 Time to Rescue	17
2.3.2 Hemodynamic Parameters	17
2.3.3 Postoperative Pain Assessment	19
2.4 Discussion	20
CHAPTER 3: ADULT ADIPOSE DERIVED MULTIPOTENT STROMAL CELLS ALTER SYSTEMIC T CELL POPULATIONS AND BIOMARKER LEVELS OF BONE METABOLISM FOLLOWING FACIAL IMPLANTATION OF BONE XENOGRAFTS IN A PORCINE MODEL	24
3.1 Introduction	24
3.2 Materials and Methods	26

3.2.1	Study Design	26
3.2.2	Animals and Husbandry	27
3.2.3	Experimental Groups	28
3.2.4	Adipose Tissue Harvest	28
3.2.5	ASC Isolation	29
3.2.6	Bioengineered Autologous Grafts	29
3.2.7	Surgical Protocol	31
3.2.8	Blood Collection	32
3.2.9	Complete Blood Counts	32
3.2.10	Serum and Plasma Cryopreservation	33
3.2.11	PBMC Isolation, Counting, and Cryopreservation	33
3.2.12	Serum Biomarker ELISAs	34
3.2.13	PBMC Preparation for Flow Cytometry Analysis	34
3.2.14	Flow Cytometry Analysis	36
3.2.15	Bone Volume and Surface Area Measurements	37
3.2.16	Statistical Analysis	37
3.3	Results	38
3.3.1	Flow Cytometry	38
3.3.2	Complete Blood Count	38
3.3.3	Serum Biomarkers	38
3.3.4	Bone Volume and Surface Area	39
3.4	Discussion	43
CHAPTER 4: DISCUSSION AND FUTURE RESEARCH		48
REFERENCES		50
APPENDIX		61
VITA		67

ABSTRACT

The use of a porcine model in assessing bone grafts in vivo is common when a large animal model is necessary. In this thesis we aimed to improve the porcine model of facial reconstruction through the use of a local anesthesia and novel methods of assessing the immune response to and bone forming ability of adult adipose derived mesenchymal stromal cells (ASC). The goals of the research were: 1) evaluate the effect of a bupivacaine mandibular nerve block on blood pressure (BP) and heart rate (HR) in response to surgical stimulation and the need for systemic analgesics postoperatively, 2) quantify circulating T and B cell populations, 3) measure serum levels of biomarker for bone metabolism; 4) assess correlations between circulating biomarkers and surgical site bone volume and surface area.

14 adult, male Yucatan miniature pigs were utilized for the studies. The anesthesia study separated the pigs equally between two groups: saline control and bupivacaine nerve block. BP and HR were monitored during surgery and a custom ethogram was used to assess pain postoperatively. The ASC study assigned the pigs to three groups: no implant (NI), bovine xenograft (S), and bovine xenograft with autogenous ASCs (ASC). Characterization of peripheral lymphocyte populations was done with flowcytometry using antibodies against porcine CD4, CD8, CD3, and CD21. Six ELISA kits for biomarkers of bone remodeling were used to measure serum levels.

The anesthesia study demonstrated improved surgical HR and BP control with a bupivacaine mandibular block in conjunction with systemic analgesics but no improvement in postoperative analgesia.

In the graft response study, the ASC group demonstrated significantly lower levels of circulating CD4+/CD8+, CD4+/CD8-, and CD3+/CD4+ lymphocyte populations. Serum levels of Carboxy-terminal cross-linked telopeptide of type I collagen were significantly elevated in the

ASC group while levels of osteocalcin were lower. Bone specific alkaline phosphatase was significantly lower in both the ASC and S groups compared to NI.

The findings in these studies help to improve how we utilize the porcine model and will help lead to a better understanding of the immune system and biomarker response in pigs.

CHAPTER 1: LITERATURE REVIEW

1.1 Adipose Derived Multipotent Stromal Cell Introduction

1.1.1 Multipotent Stromal Cell Definition and Nomenclature

The area of regenerative medicine has been very active in research in recent years. The discovery of adult multipotent mesenchymal stromal cells has taken this field of research in new directions without the stigma associated with embryonic stem cells. Multipotent mesenchymal stromal cells (MSCs) originate from different connective tissues including bone (1), adipose (2), skin (3), muscle (4), umbilical cord (5), corneal stroma (6), and periosteum (7). MSCs have recently been described as having many similarities to pericytes as they are thought to be of perivascular origin (8). This helps explain their extreme abundance in multiple tissue sources. These cells are readily available and have the ability to differentiate into multiple tissues including bone, adipose, muscle, and neural tissue (9). The International Society for Cellular Therapy proposed three minimal criteria to define human MSCs. First, plastic-adherence must be demonstrated by MSCs when maintained in standard culture conditions. Second, expression of CD105+, CD73+ and CD90+ must be present while lacking expression of CD45-, CD34-, CD14- or CD11b-, CD79 α - or CD19- and HLA-DR surface molecules. Third, trilineage differentiation in vitro must be demonstrated through differentiation into osteoblasts, adipocytes and chondroblasts (10).

The nomenclature used when discussing MSCs has been, for the most part, standardized over the last few years. Having multiple tissue sources for cells requires different nomenclature dependent upon the tissue of origin. The majority of articles are focused on stromal cells from bone marrow (BMSC) or adipose tissue (ASC). The term “multipotent mesenchymal stromal cell” is currently preferred over “adult stem cell” as these cells do not have the same

differentiating characteristics as pluripotent stem cells. When these cells are collected from tissue they are usually mixed in with other cell types. In the case of ASCs this mixture is called the stromal vascular fraction (SVF) and it consists mainly of pericytes, hematopoietic-lineage cells, ASCs, and fibroblasts (11). Purification of MSCs is usually accomplished after culturing to eliminate nonadherent cells. Culturing MSCs produces colony-forming units (CFU), used to measure cell frequency in tissues, each of which is initiated from a single MSC (12, 13).

1.2 Therapeutic Effects Of Adipose Derived Multipotent Stromal Cells

1.2.1 Differentiation Capabilities Of Adipose Derived Multipotent Stromal Cells

ASCs meet the criteria set by the International Society for Cellular Therapy in their differentiation capabilities. In vitro ASCs have demonstrated adipogenic, osteogenic, chondrogenic, and myogenic differentiation (14). Each pathway to differentiation is induced by specific culture media. Osteogenic differentiation is usually accomplished using a mixture of ascorbic acid, dexamethasone, and β -Glycerophosphate (15). Other components can be substituted or added including vitamin D3 and ascorbate-2-phosphate (11, 14, 15).

Dexamethasone induces Runx2 expression by FHL2/ β -catenin-mediated transcriptional activation and enhances Runx2 activity thus promoting osteoblast differentiation. Ascorbic acid leads to the increased secretion of collagen type I and the phosphate from β -Glycerophosphate serves as a source for the phosphate in hydroxylapatite (15). Modalities used to confirm osteogenic differentiation include: histochemical analysis using BM Purple, alizarin red, ALP assay or von Kossa stain; mRNA of BGLAP, ALP, COL1A1, or RUNX2 (14).

1.2.2 Trophic Effects Of Adipose Derived Multipotent Stromal Cells

The trophic effect of ASCs refers to their ability to promote cell growth, differentiation, and survival beyond their direct differentiation capabilities. There are a number of factors secreted

by ASCs which aid in the survival and expansion of surrounding tissues. Vascular endothelial growth factor (VEGF), hepatocyte growth factor (HGF), fibroblast growth factor (FGF-2), and transforming growth factor beta (TGF- β) are secreted by ASCs and have been shown to promote angiogenesis and wound healing (11). These mechanisms improve ASCs ability to be used in regenerative medicine. By promoting survival and growth of surrounding tissues, ASCs may improve the integration of implants and grafts into the host tissues.

1.2.3 Immune Modulatory Effects Of Adipose Derived Multipotent Stromal Cells

One of the largest hurdles to overcome in the long term survival of a graft or implant is the immune system response. The ability to completely bypass this problem using autologous tissue is not always feasible due to the limited supply and possible donor site morbidity. ASCs show great promise in addressing this issue through tissue engineering due to the ready supply and easy accessibility of adipose tissue. Immune privilege and regulation has also been demonstrated by ASCs through a multitude of secreted factors and cell-cell binding. This ability has been demonstrated clinically with the control of graft-versus-host disease (GVHD)(16-18), colitis (19), arthritis (20), and other autoimmune diseases (21).

The mechanisms by which ASCs can control the immune response are vast and depend on the application. ASCs can act on both adaptive and innate immune systems by T cell suppression, reduction in natural killer cell (NK) proliferation and cytotoxicity, promotion of regulatory T cells (T_{reg}), reducing B cell proliferation and activation, and reducing dendritic cell maturation (20, 22-24). When it comes to graft acceptance, T cells are the main target for therapy as they are the primary mediator of graft rejection.

The suppression of T cell expansion in vitro by ASCs has been well described in the literature. ASCs are believed to have anti-inflammatory and immune-modulating properties which have

been associated with inhibition of T-cell activation and possible increase in regulatory T cell (T_{reg}) numbers (20, 22, 23, 25). The suppressive effects of ASCs on T-cell populations have been consistently demonstrated on both CD4⁺ T helper (Th) cells and CD8⁺ cytotoxic T lymphocytes.(26) Cell to cell contact and release of soluble factors have been shown to attribute to ASC mediated T cell suppression (27-29). Multiple potential mediators have been identified: protoglandin E₂ (PGE₂), indoleamine-2,3-dioxgenase (IDO), nitric oxide, IL-10, IL-6, transforming growth factor-beta (TGF- β) (9, 24, 26, 30). The multitude of pathways in which ASCs modulate or suppress the immune system helps to explain why they can be advantageous in different disease processes.

1.3 Bone Remodeling And Grafting

1.3.1 Physiology And Biology Of Bone Remodeling

Bone remodeling is an ongoing process with in the skeletal structure to maintain the health and structural strength of bone. Remodeling of bone is controlled by a balance between osteoclast and osteoblast activity which resorb old, microdamaged bone and form new bone respectively. This process is continuous in healthy bone at a rate to maintain homeostasis and varies depending on bone type. Cortical bone remodels at a slower rate than trabecular bone. The process can also respond to changes in mechanical loading and demand.

Bone remodeling generally occurs in an ordered series of events: activation, resorption, reversal, and formation. Activation refers to the initial process of forming and activating multinucleated preosteoclasts and their binding to bone matrix. Osteoclasts are regulated by NF- κ B (RANKL), IL-1 and IL-6, colony stimulating factor (CSF), parathyroid hormone, vitamin D, and calcitonin (31). Hydrogen ions secreted by osteoclasts lower the pH within the bone-resorbing

compartment to help mobilize bone minerals (32). Once osteoclast bone resorption has begun it takes approximately 2 to 4 weeks, in humans, until the reversal process begins.

The reversal phase is the transition from bone resorption to bone formation. Bone resorption cavities contain monocytes, osteocytes, and preosteoblasts for new bone formation. The exact signals which trigger the transition from resorption to formation have not been identified.

Transforming growth factor beta (TGF- β) from bone matrix can inhibit RANKL production and decrease osteoclast resorption (33).

Formation of bone is carried out by osteoblasts. Bone progenitor cells, pre-osteoblasts, are located in the endosteum, periosteum, and Haversian canals. These cells are stimulated through growth factors (BMP, FGF, IGF, platelet-derived growth factor (PDGF), and interleukins) to proliferate into osteoblasts. Three stages are involved in osteoblast differentiation: proliferation, matrix maturation, and mineralization. The proliferation stage includes secretion of extra cellular matrix (ECM) proteins by osteoblasts to form non-mineralized bone matrix or osteoid. Matrix maturation occurs when the osteoid proteins are crosslinked to form a more stable structure. The crosslinked collagen type I fibrils act as templates for deposition of inorganic minerals to form the mineralized bone matrix. Calcium and phosphate are concentrated while mineralization inhibitors such as pyrophosphate or proteoglycans are destroyed (34). Once osteoblasts have become surrounded by matrix they can become embedded osteocytes, inactive osteoblasts and become bone lining cells, or undergo apoptosis. Approximately 50 to 70% of osteoblasts undergo apoptosis at completion of bone formation.

1.3.2 Bone Graft Models And Nomenclature

Bone grafts are used commonly for orthopedic defects which are at risk of not healing without intervention, commonly called critical size defects. Other terms often used are “nonhealing” or

“nonunion”. Critical size defects cannot be completely defined by size as bone is an anisotropic material and healing will vary between location, surrounding tissue damage, and use. The majority of models used to study treatment for such defects involve rodents using a calvarial defect or spinal fusion model (35). The defects are made in the parietal bone with the size varying from 4mm in mice to up to 8mm in rats (36-39). Models in larger animals can utilize the flat bones of the skull (40) or long bones (41, 42).

Grafts are categorized based on the donor species as it relates to the host. Autologous grafts are intra person grafts for which the same person is the recipient and donor. These grafts are seen as gold standard due to the lack of immune rejection. Allogeneic grafts are between two individuals of the same species. Allogeneic grafts are used commonly in humans from cadavers and carry risk of immune rejection or disease transmission. Xenogeneic grafts occur when the donor and recipient are of different species. Xenografts are associated with severe immune responses if not properly processed before implantation. If preparation of this type of graft could be perfected it would be a huge step toward alleviating the shortage of available grafts. If two individuals are identical genetically, such as inbred mice or some identical twins, a graft between them is known as syngeneic and is usually well accepted.

1.3.3 Bone Graft Healing

The ability of a bone graft to incorporate into existing tissue is dependent on three main functions of the graft material and host tissue: osteogenesis, osteoconduction, and osteoinduction.

Osteogenesis refers to the direct formation of new bone. To perform osteogenesis, a bone graft requires living cells. Osteoblasts or pre-osteoblasts must be present within the graft in order for the graft to directly contribute to osteogenesis within the recipient (43). Pre-osteoblasts are

believed to contribute more to the new bone formation if a nonvascularized graft is used. These pre-osteoblasts are found in bone marrow, periosteum and endosteum.

The ability of a graft to provide structural framework on which host cells reconstitute is known as osteoconduction (44). Union with the host bone begins with ingrowth of vessels, osteoblasts, and stem cells from the host into the graft. Structural properties which influence the osteoconductive capabilities of graft material include porosity, pore size, pore connectivity, and surface topography (45). Factors which can restrict osteoconduction are defect size, recipient bed cellularity, host resorption and remodeling, and contact with donor tissue.

Osteoinduction refers to recruitment of progenitor cells from the host tissue into the graft where they can differentiate to osteoblasts (46). This could also be defined as the process by which osteogenesis is induced. An ideal osteoinductive material will function on three key principles: 1) Recruitment of MSCs, 2) MSC differentiation to osteoblasts, and 3) Ectopic bone formation (47). Any material or graft which can display these three principles should display good osteoinduction.

All three of the previously described function would be well demonstrated by an ideal bone graft. A deficiency in one area can cause problems in a grafts ability to properly incorporate into the recipient tissue. Appropriate integration is key to having a well-tolerated and functional graft.

1.4 Serum Biomarkers Of Bone Remodeling

1.4.1 Serum Biomarkers

Research involving the treatment of bone defects is reliant on the ability to assess bone growth. Having the ability to monitor the growth of bone in a noninvasive manner allows for the collection of more data without increasing the number of animals used in research. It also allows for monitoring of treatments in humans. Noninvasive modalities in monitoring bone remodeling

include radiographs, magnetic resonance imaging (MRI), computerized tomography (CT) scans, bone scintigraphy scan, and serum biomarkers. Clinically in humans a bone density scan is done for women who are at risk for osteoporosis. Imaging modalities similar to this are very useful but carry certain risks if repeated too frequently due to the exposure to radiation with MRI being the exception. These imaging techniques can also be cost prohibitive serial images are required. Systemic biomarkers have shown promise as a method to frequently assess skeletal structural changes over time.

A serum biomarker of bone remodeling is a biologic marker detectable in the serum that may be used to measure the presence or progress of bone remodeling due to disease or treatment. The biomarkers for bone are generally molecular structures released from tissue or cells in the process of remodeling bone. The majority of markers target osteoclast or osteoblast activity and products from the breakdown or synthesis of collagen. Such biomarkers have been studied to assess bone turnover as it relates to multiple diseases: metastatic cancer involving bone, osteoarthritis, osteoporosis, primary hyperparathyroidism, and osteodystrophy to name a few (48-52). Many of the markers investigated are not useful as a single diagnostic technique, but they can be helpful in monitoring at risk patients. Tang et al reported serum levels of bone alkaline phosphatase (BAP) and type I collagen carboxyterminal telopeptide (ICTP) to be significantly higher in lung cancer patients with bone metastasis (50). The current thought is that there isn't one biomarker that is useful alone but possible patterns in multiple biomarkers may be helpful in predicting disease (53).

CHAPTER 2: THE EFFECT OF A BUPIVACAINE MANDIBULAR NERVE BLOCK ON INTRAOPERATIVE CHANGES IN BLOOD PRESSURE AND HEART RATE AND THE NEED FOR POST-OPERATIVE ANALGESICS IN A YUCATAN MINIATURE SWINE MANDIBULAR CONDYLECTOMY MODEL: A PILOT STUDY

2.1 Introduction

Animal models are a priceless resource when developing new techniques and treatments for human medical application. In some instances, the ability to improve an animal model comes from established procedures in humans. This holds especially true for the implementation of local nerve blocks. The information gathered from human patients on dose, duration and extent of pain relief provided by local nerve blocks is a basis for improved analgesia in animal models. Miniature swine are used extensively in the development of dental, oral and maxillofacial surgical techniques due to similarities to humans in anatomy, healing, and remodeling (40, 54-57). There is a lack of literature describing local anesthetic techniques in miniature pig models for oral and maxillofacial surgery, though this form of analgesia is common in human patients undergoing the same procedures (57). As with every animal surgical model, the quest for the most effective anesthetic and analgesic regimens is a top priority for animal health and well-being.

Local nerve blocks are an established and effective method for pain control in oral and maxillofacial surgical procedures (58). Their local action, prolonged analgesia and limited side effects make them an appealing alternative to systemic analgesics such as opioids. Bupivacaine (0.5%) nerve blocks alone are reported to last between 2 and 12 hours in animals and humans (59, 60). The mandibular nerve is the largest branch of the trigeminal nerve. It has both motor and sensory function, with branches innervating the muscles of mastication and mandibular teeth. The nerve exits the skull through the foramen ovale and runs cranial and ventral toward the mandibular foramen where the inferior alveolar nerve enters. The anatomy of the miniature

pig mandibular nerve has not been extensively studied but is assumed to be similar to that of other mammals (61). A local mandibular nerve block has been shown to provide relief from bone and soft tissue pain in humans and animals undergoing dental procedures (58, 62-64). A proximal mandibular nerve block eliminated the need for intraoperative analgesia and provided postoperative analgesia for 8 hours in a canine patient undergoing a rostral mandibulectomy (63). Pain relief is important both for post-operative comfort and healing. Self-trauma from licking, scratching or rubbing a surgical site in response to pain impairs healing. Stress from post-operative surgical pain has also been linked to delayed wound healing in multiple models (65, 66). Release of glucocorticoids and catecholamines as well as a decrease in local cytokines and cellular infiltrates from stress can impair wound healing (65). Improving postoperative analgesia can decrease discomfort and stress in animal surgical models.

This study utilized Yucatan miniature pigs as a model for mandibular condylectomy and implant surgery. The aim was to determine the efficacy of a 0.5% bupivacaine mandibular nerve block for intra- and postoperative analgesia in the Yucatan miniature pig model. We hypothesized that a mandibular nerve block with bupivacaine: (1) decreases the need for systemic analgesia during mandibular condylectomy and implant surgery compared to saline in a porcine model and (2) decreases postoperative signs of pain.

2.2 Materials And Methods

2.2.1 Animals And Husbandry

This study was performed at the Louisiana State University School of Veterinary Medicine , an AAALAC International accredited facility, in accordance with the *Guide for the Care and Use of Laboratory animals* (67). All experimental procedures were approved by the IACUC.

Fourteen male castrated Yucatan miniature pigs (*Sus scrofa domestica*) were certified to be free from common domestic swine diseases (leptospirosis, brucellosis, pseudorabies, transmissible gastroenteritis, porcine reproductive respiratory syndrome and toxoplasmosis) and current on *Mycoplasma hyopneumoniae* bacterin (M + Pac) vaccine by the supplier, Sinclair Bio-Resources (Columbia, MO). All pigs were skeletally mature (mean age, 24.7 months; range, 20 to 32 months). They were housed in groups of 4 to 5 in an ambient temperature facility within 124 inch by 84 inch pens with rubber padded flooring covered by about 2 inches of pine shavings (S&S Farms, Inc, Franklinton, LA). A radiant heat source was supplied when ambient temperatures decreased below 50°F (10°C). Pigs were offered Mazuri mini pig active adult diet (Land O'Lakes, Inc, Saint Paul, MN) twice daily in one trough per two pigs, and they had unrestricted access to water for the duration of the study. Pigs were allowed to acclimate to their new environment for 7 days prior to initiation of the study, and they were housed singly for about 18 hours after surgery before being returned to their established social groups.

2.2.2 Experimental Groups

All pigs underwent left mandibular condylectomy surgery as part of an implant study. Prior to the surgical procedure each pig was randomly assigned to one of two treatment groups. One cohort (n=7) received a bupivacaine mandibular nerve block while the other cohort (n=7) received an equal volume of saline at the mandibular nerve block injection site. Within each treatment cohort, condylectomies were performed on all pigs and implants were placed in six (one received a condylectomy only in each group).

Anesthesia Protocol: After 12 hours of food withdrawal, pigs were chemically restrained with ketamine (10mg/kg, Vedco Inc; St. Joseph, MO), midazolam (0.2mg/kg, Hospira, Inc; Lakeforest, IL), and dexmedetomidine (2ug/kg, Pfizer Animal Health, NY, NY) administered

intramuscularly. Fifteen minutes later, anesthesia was induced with 5% isoflurane in 100% oxygen at 1.5 L/minute flow via facial mask. When muscle relaxation characterized by loss of jaw tone and palpebral reflexes was observed, the trachea was intubated with a cuffed Murphy's endotracheal tube (7-9 mm internal diameter). Anesthesia was maintained in all pigs at a vaporizer setting of 1.5% isoflurane in a circular breathing system until the end of the surgery. Continuous heart rate (HR) and blood pressure (BP) recordings were performed perioperatively on all pigs. Blood pressure was measured in 8 pigs through an arterial line placed in the auricular artery. Arterial line placement was not possible in 6 pigs (2 from the bupivacaine group, 4 from the control group), so blood pressure was monitored with a non-invasive blood pressure (NIBP) cuff on the mid metatarsus. Data from the NIBP cuff was not included in the statistical analysis due to differences between invasive and noninvasive BP monitoring techniques.(68-70) Mean values and standard deviations were calculated from continuous BP and HR data within segments corresponding to 1 minute before the surgical incision (baseline), 1 minute prior to rescue analgesia (pre-rescue) and for 1 minute at both 10 and 20 minutes post-rescue. These readings included only the condylectomy portion of the surgery in all pigs. Data from the implant portion of the surgery were not included in the analysis.

2.2.3 Nerve Block and Rescue Analgesia

After anesthesia was induced, pigs were placed in right lateral recumbency and the left jaw prepared for surgery. Following aseptic preparation, pigs were randomized to receive a mandibular block with an equal volume of either 0.5% bupivacaine (Hospira, Inc: Lakeforest, IL) (0.4 mg/kg, *bupivacaine group*) or saline (volume based on bupivacaine calculation, *control group*). 5 mL was the average volume used. Bupivacaine was selected based on the experience of the anesthesiologist and for its longer duration of action compared to lidocaine. The person

administering the block was not blinded to treatment. For the mandibular block, an insulated 10cm, 20G needle was inserted medial to the left mandibular ramus at the point of the angle of the mandible and advanced toward the lateral canthus of the ipsilateral eye with the aid of a nerve stimulator (Pajunk, MultiStim Sensor, Germany) to identify the injection site (**Figure 1**). The nerve stimulator was set to deliver a 1 mA impulse. When movement of the mandible was noted, signaling stimulation of the muscles of mastication, the impulse was reduced to 0.4 mA. If mandibular movement was sustained at 0.4 mA the treatment was administered through the stimulator needle. Protocol for administration of the block was based on the anesthesiologist's experience and expertise.

After the mandibular block, pigs were assigned to 2 different surgical procedures involving a left mandibular condylectomy. During the surgery, a rescue analgesic protocol consisting of fentanyl (Hospira, Inc; Lakeforest, IL) and lidocaine (Sparhawk laboratories, Inc; Lenexa, KS) was instituted if BP or HR increased 20% above baseline values. For rescue analgesia, a bolus of fentanyl (5mg/kg) and lidocaine (2mg/kg) was administered followed by a continuous rate infusion (CRI) (fentanyl 7.5 µg/kg/hr and lidocaine 50 µg/kg/min) for the remainder of the procedure.

2.2.4 Surgical Procedure

Two pigs received condylectomy only (1 in each treatment group) and twelve received condylectomy and implant (6 in each treatment group). Briefly, a #10 blade was used to make a 5 cm skin incision in the left submandibular area. The incision was carried through the platysma, cervical fascia and masseter muscle with electrocautery using blunt and sharp dissection. A periosteal elevator was used to expose the ramus of the mandible from the mandibular angle to the condyle. A premeasured osteotomy from the sigmoid notch was carried ventrally to the

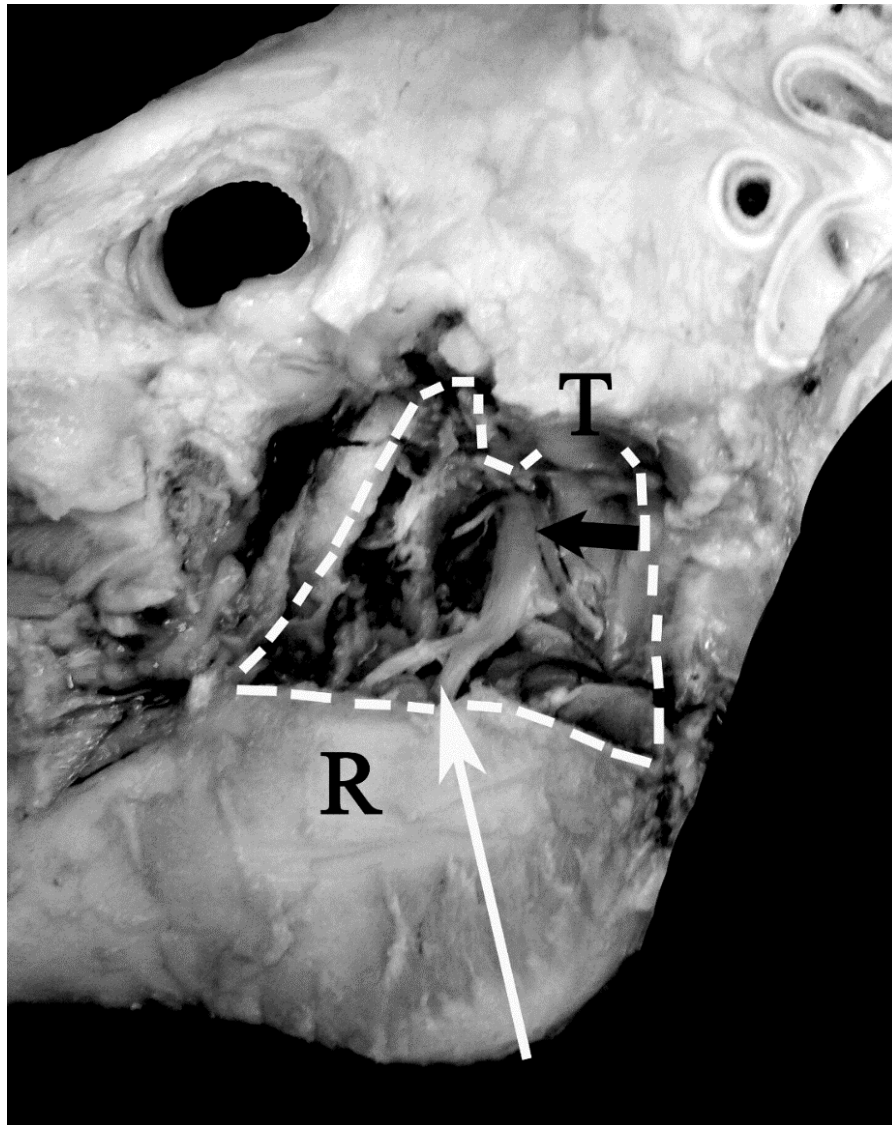


Figure 2.1 Technique for administration of nerve block: Nerve stimulation and block technique. This dissection of a pig skull demonstrates the pathway of the mandibular nerve and the point at which the block is expected to be administered. The mandibular nerve (black arrow) runs cranial ventral from the foramen ovale toward the mandibular foramen. The needle attached to the electronic nerve stimulator was advance from the angle of the mandible toward the lateral canthus of the ipsilateral eye (white arrow) and medial to the ramus of the mandible. The white dotted line indicates the edges of the removed portion of the ramus (R). The temporomandibular joint is also labeled (T).

middle of the ramus where a horizontal osteotomy was created through the caudal border with a reciprocating saw with copious irrigation. This segment of bone containing the condyle and a portion of the ramus was then removed after dissecting the medial musculature. Bone implants

similar in size and shape to the removed segment were secured in the space previously occupied by the native ramus-condyle unit with Stryker-CMF miniplates and screws. Following copious sterile saline irrigation, the masseter muscle, platysma muscle and subcutaneous tissue were closed with #2-0 synthetic monofilament absorbable suture (Biosyn, Covidien; Mansfield, MA) in respective layers. Skin edges were apposed with #2 nylon (Oasis; Mettawa, IL). All surgical procedures were performed by oral and maxillofacial surgeons with the assistance of a boarded veterinary surgeon.

2.2.5 Postoperative Pain Assessment

During recovery, pigs were monitored for signs of pain or discomfort (Table 1). Heart rate (direct auscultation), respiratory rate (visual observation), appetite, urination, defecation, ambulation, vocalization, non-purposeful movement and mentation were recorded every 15 minutes for 2 hours and then at 4 hours post extubation with first recording made at the time of extubation. Subjective assessments (vocalization, ambulation, etc.) were assigned a numeric value for statistical analysis. Time from end of surgery to extubation varied due to the need for postoperative computer tomography scans and based on duration of recovery from anesthesia. Assessment of all pigs was performed by a veterinarian who was blinded to treatment. If pigs were noted to be painful by the observer a dose of buprenorphine (Reckitt Benckiser Pharmaceuticals Inc; Richmond, VA) (30 ug/kg) was administered intramuscularly and then every 8 hours as needed. Administration of buprenorphine was not based on ethogram score but rather clinical evaluation by the veterinarian.

Table 2.1 Postoperative Pain Ethogram:

Behavior	Score					
Appetite	0 None	1 Mild	2 Moderate	3 Aggressive		
Urination	0 None	1 Urine				
Defecation	0 None	1 Feces				
Ambulation	0 Recumbant	1 Uncoordinated	2 Sluggish	3 Normal	4 Hyperactive	
Vocalization	0 None	1 Grunt	2 Whine	3 Squeal		
Non Purposeful Movement	0 None	1 Mild	2 Moderate	3 Violent		
Mentation	0 Nonresponsive	1 Obtunded	2 Dull	3 Quiet	4 Bright	5 Hyper-responsive

A custom ethogram was used to assess clinical pain in pigs postoperatively. Assessments were completed every 15 minutes for the first 2 hours after extubation with a final reading at 4 hours after extubation.

2.2.6 Statistics

Mean values and standard deviations were calculated from continuous BP and HR data within segments corresponding to 1 minute before the surgical incision (baseline), 1 minute prior to rescue analgesia (pre-rescue) and for 1 minute at 10 and 20 minutes post rescue (10 minutes post-rescue and 20 minutes post-rescue, respectively). Repeated measures analysis of variance was used to compare hemodynamic parameters between treatment groups and time points (NCSS 8 Version 8.0.13, NCSS LLC, Kaysville, Utah). Tukey's post-hoc analysis was performed to assess statistically significant differences. Time to rescue and postoperative pain scores were analyzed using a second statistical package (MYSTAT Version 12.02.00, Chicago, IL).

Student's *t* test was used to compare times to rescue and postoperative pain scores. Significance was set at $p \leq 0.05$.

2.3 Results

For purposes of this study variations in BP and HR were used to represent responses to painful stimuli (64, 71, 72). All pigs were maintained on 1.5% isoflurane throughout the procedure, received a constant intravenous fluid rate of 5ml/kg/hr, and had minimal blood loss.

2.3.1 Time to Rescue

A total of 8 pigs were included in the statistical analysis (n= 5 bupivacaine cohort; n= 3 saline cohort), all of which required rescue analgesics intraoperatively. There was no difference in time until rescue ($p=0.84$) between the bupivacaine and saline groups (Figure 2).

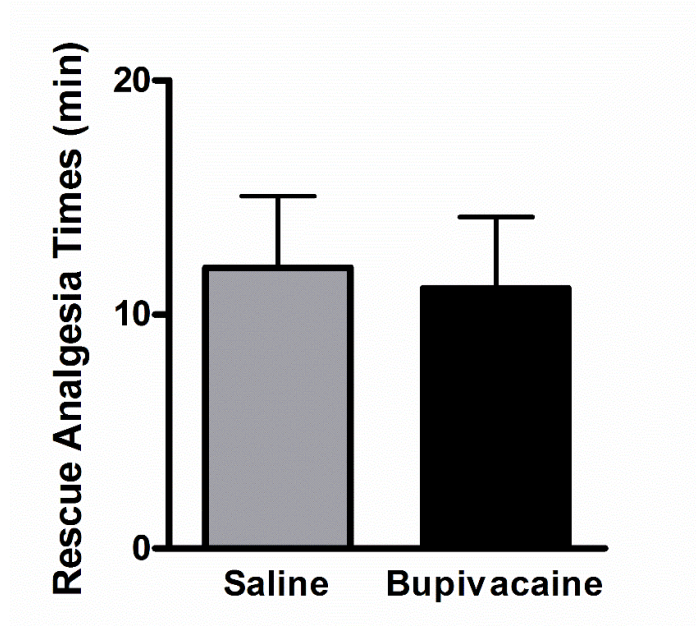


Figure 2.2: Mean \pm SEM time from start of surgery until rescue analgesics (fentanyl/lidocaine) were administered based on predetermined BP and HR changes. Differences between treatment groups were not significant ($P = 0.84$).

2.3.2 Hemodynamic Parameters

A total of 8 pigs were included in the statistical analysis (n=5 bupivacaine cohort; n=3 saline cohort). Mean BP differed significantly over time ($p = 0.002$) with the difference occurring between the baseline and the pre-rescue time points for all pigs. No difference was seen between the treatment groups overall. Within the bupivacaine group the mean pre-rescue BP was significantly higher than baseline, 10 min post, and 20 min post ($p=0.001$) (Figure 3). No differences were demonstrated between time points for the saline group.

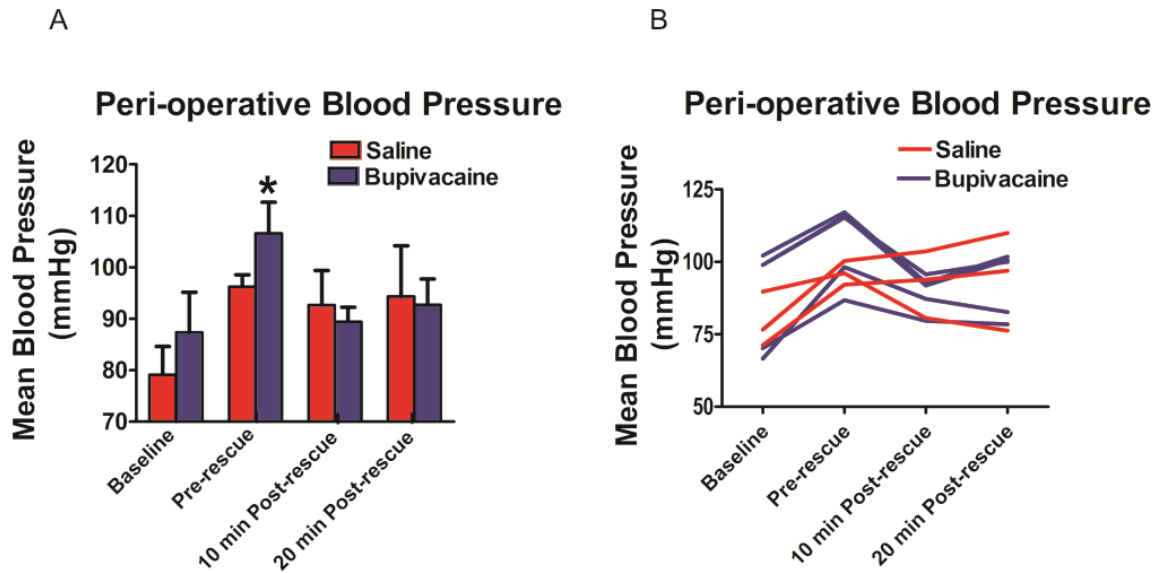


Figure 2.3: Perioperative blood pressure. (a) Mean \pm SEM BP for the two treatment groups at each of 4 time points. (b) Perioperative changes in BP by individual pig (bupivacaine group, n=5; saline group, n=3). Pre-rescue BP (*) was significantly higher from other time points within the bupivacaine group ($P = 0.001$).

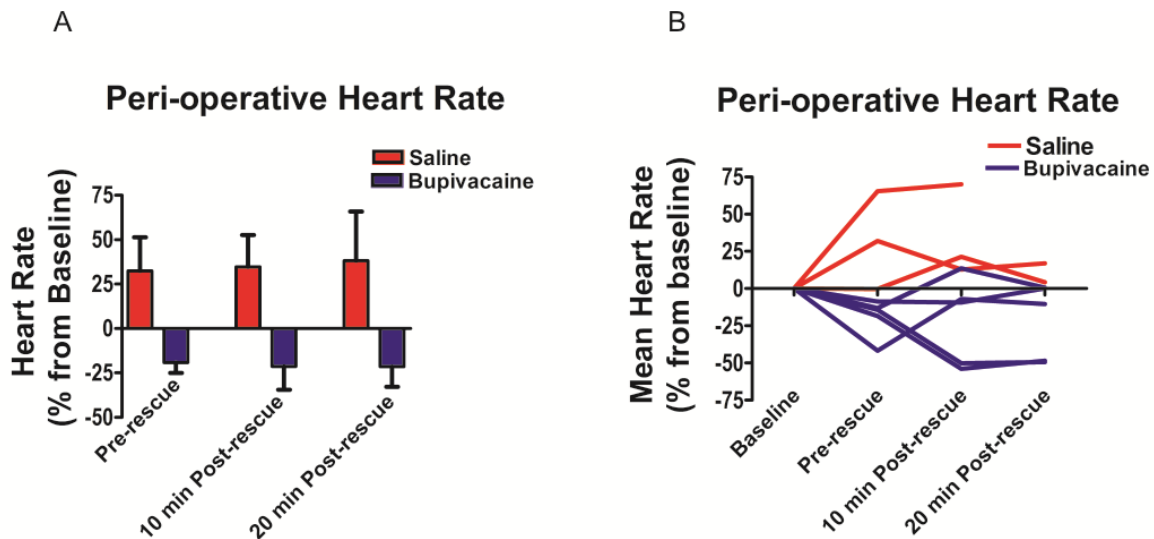


Figure 2.4: Perioperative heart rate. (a) Mean \pm SEM percent change in HR from baseline at each of 3 time points for the two treatment groups. (b) Perioperative changes in HR by individual pig (bupivacaine group, n=5; saline group, n=3). The HR was significantly lower in the bupivacaine treatment group overall ($P = 0.044$) but not at any individual time point.

On a percentage change basis, mean HR differed significantly between treatment groups ($p=0.044$) with the bupivacaine group having a lower HR than the saline group (Figure 4). Post-hoc analysis revealed no differences between time points within treatment groups.

2.3.3 Postoperative Pain Assessment

No difference was observed in postoperative parameters leading to buprenorphine injection for pain ($p = 0.13$). 4 pigs (57%) in the saline group and 6 pig (86%) in the bupivacaine group received buprenorphine injections within 3 hours of extubation (Figure 5). The only sign of pain displayed by the pigs was an unwillingness to eat and frequent motion of the mandible not associated with chewing. The two pigs which did not receive implants (split evenly between treatment groups) began eating normally within 2 hours of extubation. All pigs ate normally within 24 hours of extubation.

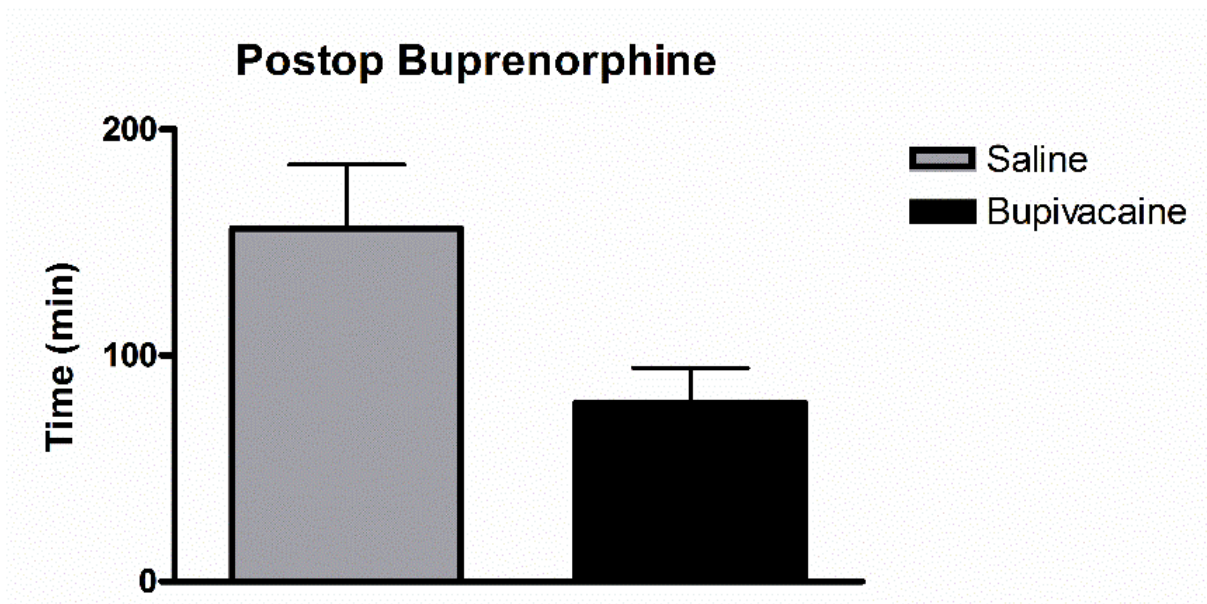


Figure 2.5: Time to buprenorphine injection after extubation. Differences between treatment groups were not significant ($P = 0.13$).

2.4 Discussion

The current study was designed to assess the efficacy of a mandibular nerve block as part of an anesthetic regimen for porcine mandibular condylectomy surgery. Addition of a bupivacaine mandibular nerve block resulted in significantly lower HR compared to a saline control at an identical level of inhalant isoflurane anesthesia and systemic fentanyl analgesia. BP was significantly reduced in the bupivacaine group after initiation of rescue analgesia while no difference was noted in the saline control. As indicated in methods, BP and HR values up to the end of the condylectomy procedure were used for statistical analysis. These findings support our first hypothesis that a bupivacaine mandibular nerve block may decrease the need of systemic analgesics during mandibular condylectomy surgery. Our second hypothesis of decreased postoperative pain was not supported by the results. Based on the combined results of this study and the common use of local blocks in human oral and maxillary surgery (58), a mandibular nerve block is justified to improve patient comfort during surgery and thereby reduce potential necessity for higher dosages of systemic analgesics.

The porcine model for oral maxillofacial surgical procedures is well established (54, 61, 73, 74). Miniature pig jaw structure closely resembles that of the human jaw in terms of bone anatomy, morphology, and healing (75). In the study reported here, the Yucatan miniature pig condylectomy model was selected for evaluation of a therapeutic intervention for temporomandibular joint disease. Animal models optimized to represent the human clinical scenario contribute to information with the highest translational value. Local anesthesia through nerve blocks of maxillary, mandibular, superficial cervical plexus, trigeminal and sphenopalatine, among others, are commonly used for human oral and maxillofacial surgery (58). Benefits in humans include improved perioperative analgesia, reduced preoperative

opioids, and lower postoperative systemic analgesics (76-78). Based on this information, we sought to improve the porcine mandibular condylectomy model with a more effective anesthetic protocol. The results achieved by addition of the block to this porcine model are similar to those reported for human patients using standard assessments of blood pressure and heart rate.

There are limitations to every animal model typically associated with size, conformation and behavior (75). While the Yucatan pig generally has optimal size, they do differ significantly from humans in several ways. Perhaps the most important are slight differences in jaw anatomy and very thick skin that are most evident when trying to identify nerve block sites. This obstacle was overcome by the use of a nerve stimulator. The use of nerve stimulation for accurate nerve localization is a feasible option for most animal research surgical facilities.

The pig's stoic nature can make post-operative pain assessment challenging. Observational signs of pain are often useful clinically but can be difficult to assess statistically. The lack of verified pain assessment signs for swine in oral and maxillofacial studies makes this process even more challenging. A custom ethogram was created specifically for the patients in this study and was based on input from multiple veterinarians with swine experience. The ethogram used did not detect a difference in behavior between groups. Increased jaw motion and reduced food consumption were the only behaviors interpreted as evidence of pain. Many of the behaviors being evaluated may have been affected by other variables besides pain itself. All variables in observational pain studies should be controlled in order to eliminate the possibility of confounding results. Evaluating the pigs from time of extubation made differentiating signs of pain and recovery from anesthesia difficult.

It is standard practice to control postoperative pain with non-steroidal anti-inflammatory drugs (NSAIDs). However, NSAIDs are controversial in research surrounding bone formation and

stem cell osteogenic capabilities since the anti-inflammatory properties have been shown to delay bone healing and stem cell differentiation (79-82). Other analgesics like opioids require frequent administration which may cause increased stress and make the animals averse to handling. Long acting regional anesthesia is a potential alternative, but there is limited published information on this approach in swine. The local nerve block seemed to improve pain control under anesthesia in combination with lidocaine/fentanyl CRI. Local nerve blocks are commonly used in human medicine for surgical procedures on the mandible and maxilla and they have been shown to improve postoperative pain management (58, 76, 77, 83-85). The increasing use of swine models for oral and maxillofacial surgical research justifies further investigation into the effectiveness of local nerve blocks.

Duration of action of local nerve blocks varies with the use of different local anesthetic drugs (86). Indwelling catheters have even been placed in humans to provide a continuous block for control of mandibular pain (87, 88). Bupivacaine reportedly provides local analgesia for 2 to 12 hours depending on the species (59, 60, 89, 90). It has been shown to be effective in relieving mandibular pain for up to 12 hours between infusions in humans when given through an indwelling catheter (87, 88). The lack of pain control postoperatively in this study may have been due to lack of duration, variation in time lapse from block to extubation, the low animal numbers, discomfort from implant, or failure of block to provide postoperative pain. The addition of drugs such as epinephrine has been shown to increase local anesthetic duration (89, 91). By adding epinephrine or utilizing a long acting local anesthetic such as liposomal bupivacaine, the duration of the local block may increase and be evident in the postoperative period.

The mandibular nerve block is a simple addition to the anesthetic regimen in the miniature pig condylectomy model that may improve analgesia. While locally blocking the mandibular nerve improved surgical analgesia in this study, a bupivacaine nerve block should not be the sole means of pain management. Systemic analgesics are required for proper pain control. Further studies and larger animal numbers are needed to better assess the intraoperative and post-operative effects of a mandibular nerve block in the porcine mandibular condylectomy model.

CHAPTER 3: ADULT ADIPOSE DERIVED MULTIPOTENT STROMAL CELLS ALTER SYSTEMIC T CELL POPULATIONS AND BIOMARKER LEVELS OF BONE METABOLISM FOLLOWING FACIAL IMPLANTATION OF BONE XENOGRAPTS IN A PORCINE MODEL.

3.1 Introduction

Adult multipotent stromal cells (MSC) are a central component of regenerative medicine, including the area of bone generation(92). Adipose tissue is an easily accessible and plentiful source of MSCs, adipose-derived multipotent stromal cells (ASCs) that has a number of advantages over bone marrow including higher MSC density and greater plasticity (2, 11, 93-95). Implants composed of ASCs on biocompatible scaffolds provide an appealing alternative to address limited supplies and potential complications of autologous and autogenous bone graft tissues. Scaffolds are generally composed of materials with compositions and microarchitectures designed to recreate the target tissue microenvironment (96-98). Following cell loading onto the scaffolds, culture environments are created to direct undifferentiated cell commitment to the target tissue lineage (99). At present, there are a number of proposed mechanisms by which scaffolds with cells demonstrate better in vivo osteogenesis than those without (100). Table 3.1 is a reference for all acronyms used in this manuscript.

Serum biomarkers are used to detect and quantify bone resorption, deposition and cell metabolic activity characteristic of conditions like menopause, neoplastic bone metastasis, and osteoarthritis (48, 50, 51, 101) A number of bone biomarkers have been validated for use in large animal models, including porcine (51). To date, use of the biomarkers to evaluate alterations in bone activity mediated by ASCs implantation has not been extensively tested. Use of biomarkers may provide a valuable mechanism to compare alterations by cell therapies for a number of clinical targets, including bone healing and deposition.

Table 3.1 Acronyms

Acronyms	
APC	Antigen Presenting Cell
ASC	Adipose Derived Multipotent Stromal Cell
BAP	Bone Specific Alkaline Phosphatase
BMP	Bone Morphogenic Protein
CBC	Complete Blood Count
CPII	C-propeptide of type II collagen
CS 846	Chondroitin sulfate epitope 846
GVHD	Graft-vs-host disease
ICTP	C-terminal telopeptide of type I collagen
IDO	Indoleamine 2,3-dioxygenase
IL-(#)	Interleukin
PYD	Pyridinoline cross links
MHC	Major Histocompatibility Complex
MSC	Multipotent Stromal Cells
NI	No implant
TNF- β	Transforming Growth Factor Beta

Recent information supports that ASCs modulate the immune response to graft materials and improve integration of foreign materials into recipients (102, 103). ASCs are reported to suppress T and B cell activation by a number of mechanisms (16, 24, 35, 104, 105). Xenogeneic transplants result in T cell stimulation due to presentation of donor major histocompatibility complex (MHC) molecules by antigen presenting cells (APC) from either the recipient (indirect) or the donor (direct) (103). Research has largely focused on ASC alteration of the local response to xenogenic material in vitro and in vivo (106, 107). Systemic immune effects of ASCs are suggested by their effective use for treatment of graft-versus-host and auto-immune diseases (16)(17, 18, 108)(19, 21). However, the ability of ASCs to effectively “mask” xenogeneic implant materials from the immune system based on a systemic response is largely unexplored (16). Enhanced osteogenic capabilities conferred by graft materials like growth factors, cell signals, and structural support are diminished by active immune response to the implant (44, 103). It is also possible that sensitization resulting from local reaction to foreign graft materials

may reduce efficacy and safety of subsequent implant administration. Mechanisms to reduce the systemic response to graft materials will increase options, improve outcomes and reduce safety concerns.

This series of investigations was designed to evaluate the systemic effects of ASC implantation on custom bone xenografts in a Yucatan miniature swine mandibular condylectomy model. The mandibular condyle was extracted or replaced with custom, deproteinated bovine corticocancellous bone grafts with or without autologous ASCs. Blood samples were collected before and up to 6 months after surgery and serum levels of bone biomarkers were quantified. Relative percentages of Cytotoxic T cells, T helper cells, and B cells were determined based on cell surface expression of CD3, CD4, CD8, and CD21. The hypothesis tested was that implantation of xenogeneic bone implants with autologous ASCs: (1) will decrease the circulating recipient T cells post-implantation compared to deproteinated xenograft alone; (2) will alter the levels of serum biomarkers of osteogenesis consistent with improved bone formation compared to no implant and deproteinated xenograft; (3) will increase the surface area and bone volume at the surgical site compared to no implant and a deproteinated xenograft alone.

3.2 Materials and Methods

3.2.1 Study Design

Fourteen pigs were assigned to one of three treatment cohorts prior to mandibular condylectomy: no implant; bovine corticocancellous implants and custom corticocancellous bone graft with autologous ASCs. Culture expanded ASCs from subcutaneous adipose tissue were seeded onto bovine cancellous xenografts machined in the shape of the mandibular condyle derived from computed tomography images. Constructs were maintained in a bioreactor culture system. Serum and peripheral blood mononuclear cells (PBMCs) were isolated from blood samples

collected at regular intervals up to 6 months after surgery. Serum and PMNCs were cryopreserved and subsequently, systemic lymphocyte phenotypes percentages were quantified with flow cytometry and biomarker levels were determined with commercially available enzyme linked immunosorbant assays (ELISA's). Bone volume and surface area was measured on 3-D reconstructions generated from computed tomography scans.

3.2.2 Animals and Husbandry

This study was performed at the Louisiana State University School of Veterinary Medicine, an Association for Assessment and Accreditation of Laboratory Animal Care (AAALAC) International accredited facility, in accordance with the Guide for the Care and Use of Laboratory Animals. All experimental procedures were approved by the Institutional Animal Care and Use Committee.

Fourteen male castrated Yucatan miniature pigs (*Sus scrofa domestica*) were purchased and certified to be current on *Mycoplasma hyopneumoniae* bacterin (M + Pac) vaccine and free from common domestic swine diseases (leptospirosis, brucellosis, pseudorabies, transmissible gastroenteritis, porcine reproductive respiratory syndrome and toxoplasmosis) by the supplier, Sinclair Bio-Resources (Columbia, MO). All pigs were skeletally mature upon arrival at the institution (mean age, 24.7 months; range, 20 to 32 months). They were housed in groups of 4 to 5 in an ambient temperature facility. Pens in which they were housed measured 124 inch by 84 inch with rubber padded flooring covered by about 2 inches of pine shavings (S&S Farms, Inc., Franklinton, LA). A radiant heat source was supplied when ambient temperatures dropped below 50°F (10°C). Pigs were offered Mazuri® Mini Pig Active Adult #5Z91 diet (Land O'Lakes, Inc., Saint Paul, MN) twice daily in one trough per two pigs, and they had unrestricted access to water for the duration of the study. Pigs were allowed to acclimate to their new

environment for 7 days prior to initiation of the study, and they were housed singly for approximately 18 hours after surgery before being returned to their established social groups.

3.2.3 Experimental Groups

All pigs were scheduled to undergo a left mandibular codylectomy procedure. Prior to surgery, pigs were blindly assigned to one of three treatment groups: no implant (Control), bovine cancellous bone scaffold only (Scaffold), and bovine cancellous bone scaffold with autologous ASCs (ASC). Pigs assigned to the Cell group had subcutaneous adipose tissue harvested from their dorsums for adult mesenchymal cell collection.

3.2.4 Adipose Tissue Harvest

Supra-gluteal subcutaneous adipose tissue was aseptically harvested with pigs under general anesthesia. Pigs were premedicated (Telazol® (Zoetis, Kalamazoo, MI), 2mg/kg intramuscularly) and after 20 minutes anesthesia was induced with isoflurane (MWI, Boise, ID) via face mask followed by maintenance with isoflurane via endotracheal tube in a semi-closed rebreathing circuit.. Pigs were positioned in sternal recumbency and the dorsal lumbar area was clipped and aseptically prepared by alternating chlorhexidine and ethyl alcohol scrubs.

Approximately 15 ml of adipose tissue was sharply excised through each of two paralumbar skin incisions approximately 5 cm from midline. Hemostasis was maintained with electrocautery.

Following tissue harvest, incision sites were thoroughly lavaged with saline. Skin was approximated with #2 polydioxanone (PDS, Ethicon, US) in a simple continuous subcutaneous/subcuticular suture pattern. Interrupted skin sutures of #1 nylon (Ethilon®, Ethicon, US) were then placed and the incision was sealed with tissue adhesive (Vetbond™, 3M, US). Incision sites were covered with iodine impregnated adhesive drapes (Ioban™, 3M) prior to recovery.

3.2.5 ASC Isolation

ASCs were isolated as previously described (109). Briefly, adipose tissue was minced with metzenbaum scissors, washed and agitated with phosphate-buffered saline (PBS). The tissue was digested in filtered PBS solution containing 1% bovine serum albumin (BSA) and 0.1% of collagenase with continuous shaking for 50 minutes. Subsequently samples were centrifuged at 300 g for 5 minutes. Samples were again agitated and centrifuged. The supernatant was removed and the stromal-vascular fraction (SVF) pellet was resuspended in 10mL stromal medium (Dulbecco's Modified Eagle Medium/Ham's F-12 Nutrient Broth (1:1), fetal bovine serum (FBS), and Penicillin/Streptomycin/Fungizone). Samples were again agitated and centrifuged. Supernatant was aspirated off leaving 5 ml of medium on each pellet. Pellets were resuspended in a total of 105 ml stromal media per 100 ml of adipose tissue digest.

3.2.6 Bioengineered Autologous Grafts

Cells were plated in cell culture flasks at a concentration of approximately 35 ml per 225cm² flask. Media was changed after 24 hours to wash away non-adherent cells and replaced with expansion medium (stromal medium with the addition of human epidermal growth factor (rhEGF), recombinant human fibroblastic growth factor (rhFGF), and transforming growth factor beta-1 (TGF- β 1)). The expansion media was changed every 3 days until day 7 to complete one passage. After each passage the expansion media was aspirated off and flasks were washed gently with 20 ml PBS. 8 ml of trypsin/T225 was added and the flask was incubated for 5 minutes at 37°C. After incubation, 8 ml of stromal medium was added to inactivate trypsin. 16 ml of trypsin/stromal medium was collected and centrifuged at 300 g for 5 minutes. Medium was aspirated off. Cells were passaged 3 times.

Bone implants were prepared using a method previously described (97). Briefly, trabecular bone was collected from the distal femur of calves and lathed into cylinders. A computer tomography (CT) image of the skull of each pig was taken (Figure 3.1). A 3D reconstruction of the skull was made from the CT images using Mimics 9.0 and MasterCam computer-aided-manufacturing (CAM) was used to design and fabricate a scaffold and bioreactor chamber. Implant fabrication was done using a Bridgeport three-axis computer-numerical-control milling machine.

Grafts were decellularized using, in order, a combination of; high-velocity streams of water, 1 hour wash in PBS with 0.1% EDTA, washes in hypotonic buffer (10mM Tris, 0.1% EDTA) overnight at 4°C, detergent (10mM Tris, 0.5% SDS) for 24 hours at room temperature, and enzymatic solution (50 units/mL DNase, 1 units/mL RNase, 10mM Tris) for 3-6 hours at 37°C. Grafts were then rinsed repeatedly with PBS and freeze-dried. Prior to seeding cells, grafts were sterilized in 70% ethanol for 1 hour, rinsed in PBS, and incubated in culture medium overnight. Cell seeding was done using previously collected ASCs suspended in culture medium at a

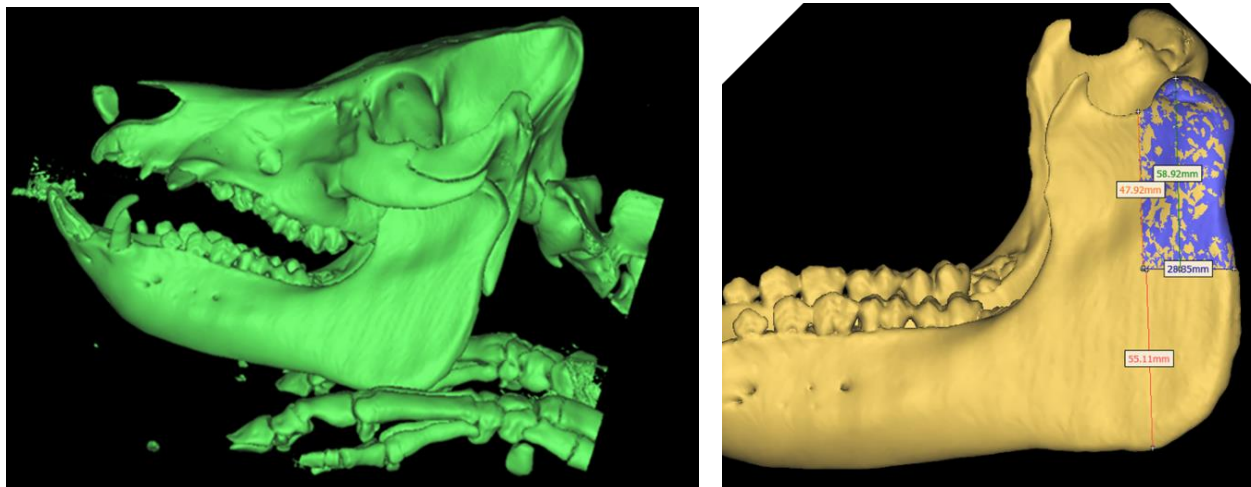


Figure 3.1 3 Dimensional Reconstruction: The CT images take at the beginning of the study were used to construct the cancellous implants. The portion of the ramus and condyle to be removed and replaced with an implant is stipled in purple.

density of 10^6 cells per ml. Grafts were suspended in cell suspension for 1 hour at 37°C while suspension was stirred at 300 rpm. Grafts were then placed into osteogenic medium, with daily medium changes. After 7 days, grafts were placed into custom bioreactor chambers and perfused at 1.8 ml/min for 4 weeks. Media was changed at a rate of 50% every 3 days.

3.2.7 Surgical Protocol

Pigs were chemically restrained with ketamine (10mg/kg, Vedco Inc.; St. Joseph, MO), midazolam (0.2mg/kg, Hospira, Inc.; Lakeforest, IL), and dexmedetomidine (2ug/kg, Pfizer Animal Health, NY, NY) administered intramuscularly. Fifteen minutes later, anesthesia was induced with 5% isoflurane in 100% oxygen via facial mask. When muscle relaxation characterized by loss of jaw tone and palpebral reflexes was observed, the trachea was intubated with a cuffed Murphy's endotracheal tube (7-9 mm internal diameter). Anesthesia was maintained in all pigs with isoflurane in a circular breathing system until the end of the surgery. Pigs were monitored throughout the procedure by a boarded veterinary anesthesiologist. Pigs were placed in right lateral recumbency and the left jaw surgically prepped with alternating scrubs of chlorhexidine and 70% isopropyl alcohol and draped. Two pigs received condylectomy only and twelve received condylectomy and implant (6 in each treatment group). Briefly, a #10 blade was used to make a 5 cm skin incision in the left submandibular area. The incision was carried through the platysma, cervical fascia and masseter muscle using blunt and sharp dissection. A periosteal elevator was used to expose the ramus of the mandible from the mandibular angle to the condyle. A premeasured osteotomy from the sigmoid notch was carried ventrally to the middle of the ramus where a horizontal osteotomy was created through the caudal border with a reciprocating saw with copious irrigation. This segment of bone containing the condyle and a portion of the ramus was then removed after dissecting the medial

musculature. Bone implants similar in size and shape to the removed segment were secured in the space previously occupied by the native ramus-condyle unit with two 1.7mm titanium Lorenz bone miniplates (Stryker, US) and 8 screws (range 6-12mm). Following copious sterile saline irrigation, the masseter muscle, platysma muscle and subcutaneous tissue were closed with #2-0 synthetic monofilament absorbable suture (Biosyn, Covidien; Mansfield, MA) in respective layers. Skin edges were apposed with #2 nylon (Oasis; Mettawa, IL). Incision sites were covered with iodine impregnated adhesive drapes (Ioban™, 3M) prior to recovery.

3.2.8 Blood Collection

Venous blood (30 mL) was collected from the cranial vena cava of each pig pre-operatively, once weekly for first 4 weeks after surgery and then every 3 weeks thereafter until the end of the study (Table 3.2). Baseline blood samples were collected when pigs were chemically restrained for surgery. Postoperative blood was collected under chemical sedation using Telazol® at a dosage of 2 mg/kg given intramuscularly. All blood was collected by pre-caval blood collection technique while pigs were dorsally recumbent with an 18g, 1.5” needle. Blood samples were divided equally by value between EDTA tubes, lithium heparin tubes, and serum separator gel tubes.

3.2.9 Complete Blood Counts:

Blood collected into an EDTA tube was supplied to the clinical pathology department at the Louisiana State School of Veterinary Medicine. The blood was analyzed within 6 hours of being collected. An ADVIA 120 (Siemens, Tarrytown, NY) was used for the initial hematology using veterinary specific software. Differentials were manually calculated from a 100 cell sample.

Table 3.2 Blood Collection

Pre-op	1	2	3	4	7	10	13	16	19	22	25
Flow	Flow	Flow	Flow	Flow	Flow	Flow	Flow	Flow	Flow	Flow	Flow
ELISA	ELISA	ELISA	ELISA	ELISA	ELISA	ELISA	ELISA	ELISA	ELISA	ELISA	ELISA
CBC	CBC	CBC	CBC	CBC	CBC	CBC	CBC	CBC	CBC	CBC	CBC

Blood collection timeline by weeks. Blood was used for flowcytometry (Flow) at each blood draw. Blood was used for analysis of bone biomarkers (ELISA) approximately every 3 weeks.

3.2.10 Serum and Plasma Cryopreservation

Serum separator gel tubes were allowed to sit for 30 minutes for blood samples to clot before centrifugation. Both lithium heparin and serum separator gel tubes were placed into a centrifuge and spun for 10 minutes at 1,000 x g (gravity). Serum and plasma samples were pipetted from their respective tubes and placed in labeled vials. The vials were placed in to an alcohol free controlled rate -1°C/minute cell freezing container (CoolCell®, biocision) in a -80°C freezer. After 24 hours, were transferred to liquid nitrogen storage.

3.2.11 PBMC Isolation, Counting, and Cryopreservation

PBMCs were isolated, counted, and cryopreserved using a previously described method (110). EDTA tubes were centrifuged for 10 minutes at 1,000 x g. After centrifugation the buffy coat was pipetted out of the tubes, along with approximately 3 mL of red cells and serum, and placed into a 15mL graduated tube. An equal volume of FBS was added to the sample and mixed well. Blood mixture was carefully pipetted on top of 3 mL of Ficoll-Hypaque (GE, Piscataway,NJ) solution in a separate 15mL tube. The tube was then centrifuged at 400 x g for 30 minutes. After centrifugation, the buffy coat (PBMC layer) was transferred by pipette to a new 15mL tube and washed with approximately 10mL of PBS. The tube was centrifuged again at 400 x g for 10 minutes. Thereafter, the supernatant was removed and cells were resuspended in 5mL of red cell lysis buffer for 3 minutes. Tubes were then filled with PBS and centrifuged at 400 x g for 10

minutes. Supernatant was removed and 10mL of PBS was added to tubes. Cells were then resuspended for counting of viable PBMCs.

10 uL of PBMC suspension was placed into a 500uL culture tube. 90 uL of 0.4% trypan blue stain was added and mixed by pipetting thoroughly. A hemocytometer was loaded with 10uL of the stained cells and PBMCs were counted at 40x magnification for calculation of PBMCs/ml.

The PBMC suspension was centrifuged again and supernatant was removed. Cells were diluted in 90% PBS and 10% DMSO solution to a concentration of no greater than 1×10^7 cells/ml.

Cell suspensions were pipetted into cryopreservation tubes which were placed in a CoolCell and put in a -80°C freezer for cryopreservation. After 24 hours, tubes were transferred to liquid nitrogen storage.

3.2.12 Serum Biomarker ELISAs

Serum samples were removed from -80°C freezer and allowed to thaw at room temperature prior to running ELISAs. Commercially available ELISA kits were purchased to analyze serum biomarker levels (Table 3.3). All kits had been previously validated for use in swine (51).

Instructions and reagents provided in kits were used for serum analysis. Plates were read on a Synergy HT Multi-Mode microplate reader (BioTek, Winooski, VT) at recommended settings. Manufacturer's instructions are provided in the appendix section (additional files 1-6).

3.2.13 PBMC Preparation for Flow Cytometry Analysis

Cryopreserved PBMCs were thawed as previously described. Briefly, cryovials were removed from -80°C freezer and placed into 37°C bead bath. Cell suspension was then transferred to 15cc tube and thawing media (90% RPMI (Roswell Park Memorial Institute) Media (Sigma-Aldrich, St. Louis, MO), 10% FBS (fetal bovine serum)) was slowly added over time with a pipette. The tube was centrifuged and cells were washed in 10mL of RPMI. After a second centrifugation

Table 3.3 ELISA Kits used for assessment of serum biomarkers of bone remodeling.

ELISA Kit	Biomarker Measured
N-MID Osteocalcin ELISA (Immunodiagnostic Systems, Scottsdale, AZ)	Osteocalcin
CPII ELISA (IBEX Pharmaceuticals Inc., MONT-ROYAL, Quebec)	C-propeptide of type II collagen (CPII)
CS 846 ELISA (IBEX Pharmaceuticals Inc., MONT-ROYAL, Quebec)	Chondroitin Sulfate epitope 846 (CS 846)
MicroVue BAP ELISA (Quidel Corp., San Diego, CA)	Bone Specific Alkaline Phosphate (BAP)
MicroVue Serum PYD EIA (Quidel Corp., San Diego, CA)	Pyridinoline cross links (PYD)
UniQ ICTP EIA (Orion Diagnostica, Finland)	C-terminal Telopeptide of Type I Collagen (ICTP)

cells were resuspended in FBS and cell concentration was determined as previously described.

Four directly conjugated antibodies were purchased for PBMC surface marker labeling with flow cytometry. Antibodies used include; PerCP-Cy 5.5 Mouse Anti-Pig CD4a (BD Biosciences, San Jose, CA), FITC Mouse Anti-Pig CD3 ϵ (BD Biosciences, San Jose, CA), PE Mouse Anti-Pig CD8a (BD Biosciences, San Jose, CA), and APC Mouse Anti-Human CD21 (BD Biosciences, San Jose, CA). PBMCs were labeled with the following procedure. Equal amounts of each sample (5×10^5 cells) were diluted into 300 μ L of PBS. Each sample had an unlabeled control tube (no antibodies) and a sample tube for antibody labeling. One μ L of each antibody solution was pipetted into the sample tubes (except CD21, 5 μ L was used). All tubes were incubated in the dark for 20 minutes. After incubation, each tube was washed with 2mL PBS followed by centrifugation for 5 minutes. The supernatant was removed and 30 μ L of 1% formalin was added to each tube. All tubes were placed in 4 $^{\circ}$ C fridge until processing. Processing occurred within 24 hours of fixation.

3.2.14 Flow Cytometry Analysis

Samples were acquired on a FACS Calibur flow cytometer (BD Biosciences, San Jose, CA) utilizing a 488 nm argon-ion laser and a 635 nm red diode laser and configured for FITC, PE, PerCP-Cy5.5 and APC fluorescence measurements using log amplification. Samples were acquired on a Macintosh G5 workstation (Apple Computer, Cupertino, CA) running Cellquest Pro software (BD Biosciences, San Jose, CA). Cell debris was eliminated by gating on intact cells based on dot plots of forward scatter versus side scatter. Dual fluorescence analyses in the form of dot plots were illustrated using Cellquest Pro software (BD Biosciences, San Jose, CA). Percentages of cells expressing CD3+, CD4a+, CD8a+, and CD21+ subsets were determined for each sample based on comparisons with negative controls. Samples were tagged with all 4 antibodies at the same time. Figure 3.1 and Table 3.4 explain the cell phenotypes associated with the evaluated surface markers. All values were normalized by division of postoperative values by the preoperative value.

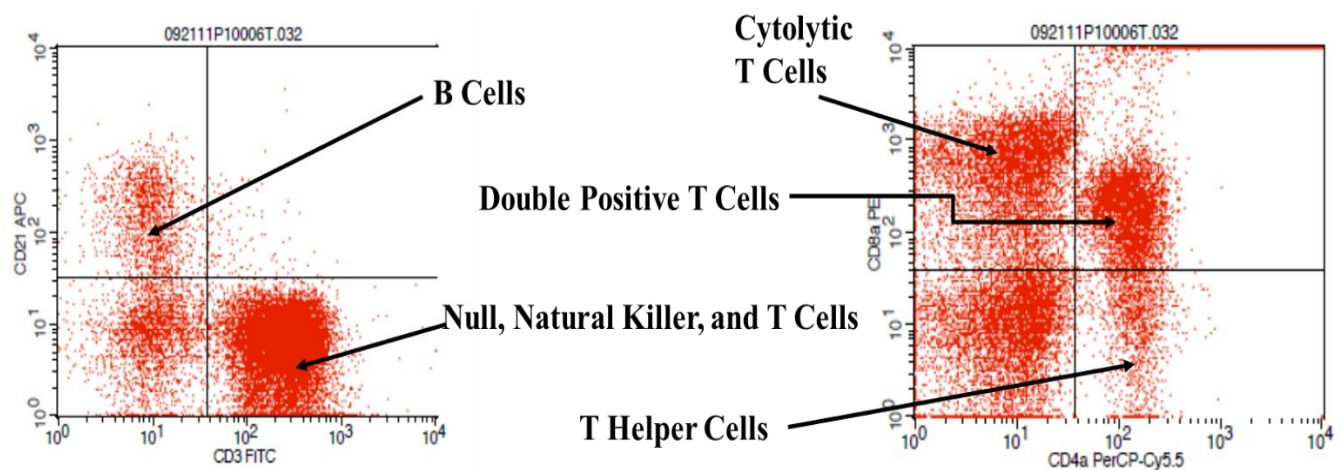


Figure 3.1 Cell Sorting by Flow Cytometry:

Table 3.4 Cell Phenotypes

Cell Markers	Cell Type
CD 4+/8-	T helper cells
CD 4-/8+	Cytolytic T cells
CD 4+/8+	Cytolytic and T helper cells
CD 3-/21+	B cells

3.2.15 Bone Volume and Surface Area Measurements

Computer tomography scans were completed on the head of each pig at 5 time points:

preoperative, postoperative, 6 weeks, 3 months, and 6 months postoperative. 4 pigs (2 from ASC and 2 from scaffold group) did not receive 6 month postoperative CTs. Digital 3D reconstruction of the skull was done using Mimics x64 version 15.01 (Materialise, Plymouth, MI). The left mandible was isolated for evaluation of volume and surface area. The evaluated area was defined by a vertical line at the caudal aspect of the last molar to the caudal edge of the mandible. Volume and surface area measurements were normalized to preoperative values for analysis by subtracting postoperative time point measurements from peroperative measurements.

3.2.16 Statistical Analysis

Flow cytometry results were analyzed for 9 combinations of cell markers: CD3+/CD21-; CD3-/CD21+; CD3-/CD21-; CD4+/CD3+; CD4+/CD8+, CD4+/CD8+; CD4+/CD8-, CD4-/CD8+.

Repeated measures analysis of variance (RMANOVA) in a mixed effects model was used to compare raw and normalized percentages of cell populations between treatment groups and time points. Fixed effects included treatment, time, and the treatment by time interaction. The random effect was pig within treatment group. Raw and normalized serum biomarker levels were analyzed using RMANOVA. Data was normalized by dividing each time point by baseline. To stabilize variance terms, CS846 and CPII values were natural log transformed and

also assessed. Bone surface area and volume were normalized to preoperative levels and evaluated using RMANOVA. Correlations between biomarker levels and bone volume, surface area (SA), and volume:SA ratio measurements were run using Spearman and Pearson Correlation Coefficients, as appropriate. Significance was set at $p \leq 0.05$. Statistical analysis was performed using SAS version 9.3 (SAS Institute, Cary, NC) Mixed and Corr procedures.

3.3 Results

3.3.1 Flow Cytometry

The effect of treatment on lymphocyte percentages was significant with all time points considered together (Table 3.4). The ASC cohort had significantly lower percentages of Th cell immunophenotypes CD4+/8-, CD4+/8+, and CD3+/4+ when compared to the scaffold cohort (Figure 2). The NI group had significantly lower percentages of Th cell immunophenotypes CD4+/8- and CD4+/8+ than the scaffold cohort (Figure 3.2).

3.3.2 Complete Blood Count

No significant differences were demonstrated between treatments or time points for lymphocyte, neutrophil, or total white blood cell counts.

3.3.3 Serum Biomarkers

The effect of treatment on serum biomarker levels was significant with all time points considered together (Table 3.6). Both ASC and scaffold groups had higher levels of BAP than the NI group. ICTP was higher in the ASC group than both the scaffold and NI groups. Osteocalcin levels were lower in the ASC group than NI (Figure 3.3).

3.3.4 Bone Volume and Surface Area

Normalized bone SA and volume demonstrate differences among treatments when all time points are considered together.. Volume was significantly lower in the NI group compared to the ASC group ($p=0.0041$) (Figure 3.4 B). Surface area was significantly lower in the NI group compared to both ASC and scaffold groups ($p<0.0001$) (Figure 3.4 A). No differences were demonstrated between ASC and scaffold groups. No significant correlations were demonstrated between serum biomarker values and bone volume or surface area measurements.

Table 3.5: Normalized Cell Population Differences by Treatment

Cell Population	Treatment Differences	P Value
CD 3-/21-	ASC > NI	0.0452
CD 3+/4+	ASC < S	0.0007
CD 4-/8-	ASC > NI, S	0.0009
CD 4+/8-	S > ASC, NI	0.0248
CD 4+/8+	S > ASC, NI	0.0062

T cell subset populations were evaluated in peripheral blood by flow cytometry. Cell populations were normalized to equivalent base line value and evaluated for differences. Statistical significance was set at $p\leq 0.05$.

Table 3.6: Normalized Biomarker Differences by Treatment

Biomarker	Treatment Differences	P Value
BAP	NI > S, ASC	0.0008
ICTP	ASC > S, NI	0.0129
Osteocalcin	ASC < NI	0.0179

Biomarker levels in serum were evaluated by commercially available ELISA kits. Serum levels were normalized to equivalent base line values and evaluated for differences. Statistical significance was set at $p\leq 0.05$.

Significant Normalized Cell Populations

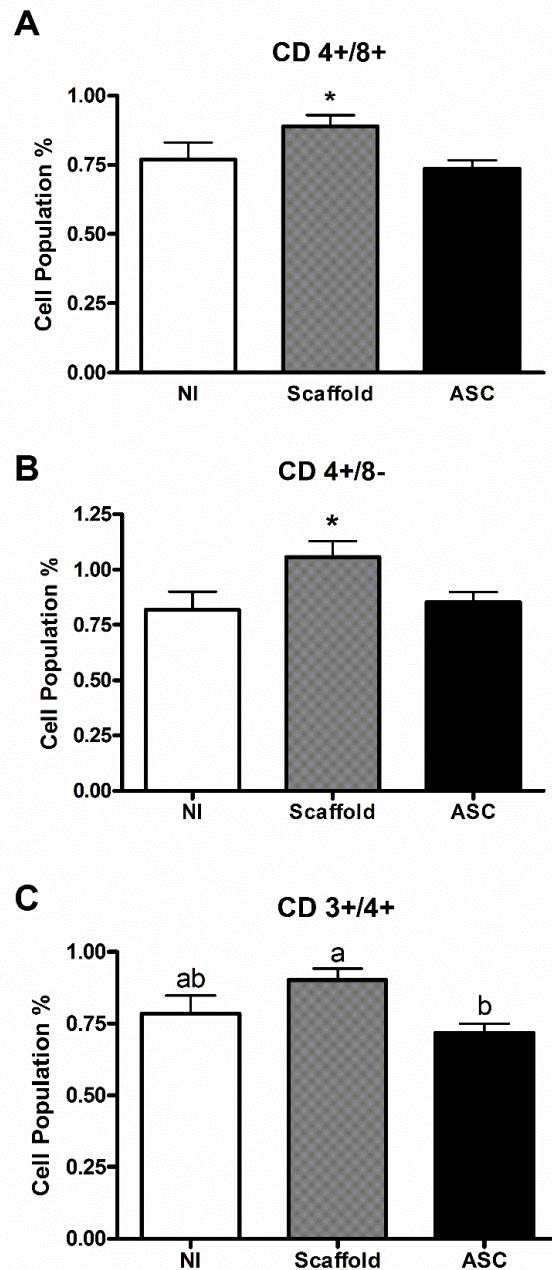


Figure 3.2 Significant differences in normalized T cell populations by treatment. Peripheral T cell subset populations were evaluated using flow cytometry between 3 treatment groups; No implant (NI), Scaffold, and Adipose Stromal Cells (ASC). Raw data was normalized to equivalent base line values. Statistical differences are denoted with an asterisk (*) or letters symbolizing if a difference was only seen between 2 of the 3 treatment groups. Statistical significance was set at $p \leq 0.05$ and error bars represent SEM.

Normalized ELISA Data

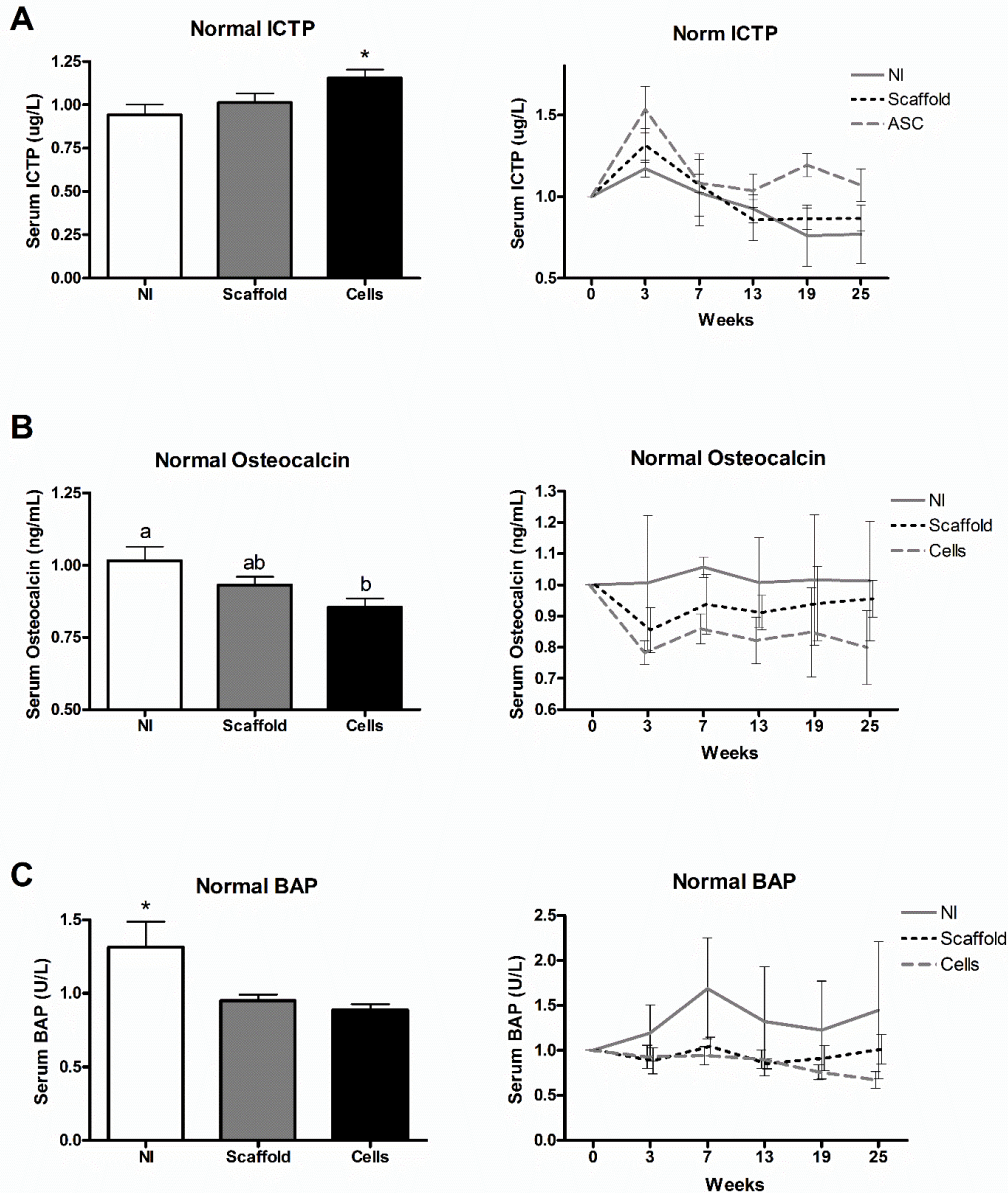


Figure 3.3: Significantly different normalized serum biomarker levels between treatments. Serum biomarker levels were evaluated using commercially available ELISA kits. Raw data was normalized to equivalent base line values. Differences between treatments is denoted with an asterisk (*). The bar graphs depict mean value over all time points by treatment groups. The line graph shows variation in biomarker levels over time by treatment among which there were no significant differences. Statistical significance was set at $p \leq 0.05$ and error bars represent SEM.

Normalized Surface Area and Volume Measurements

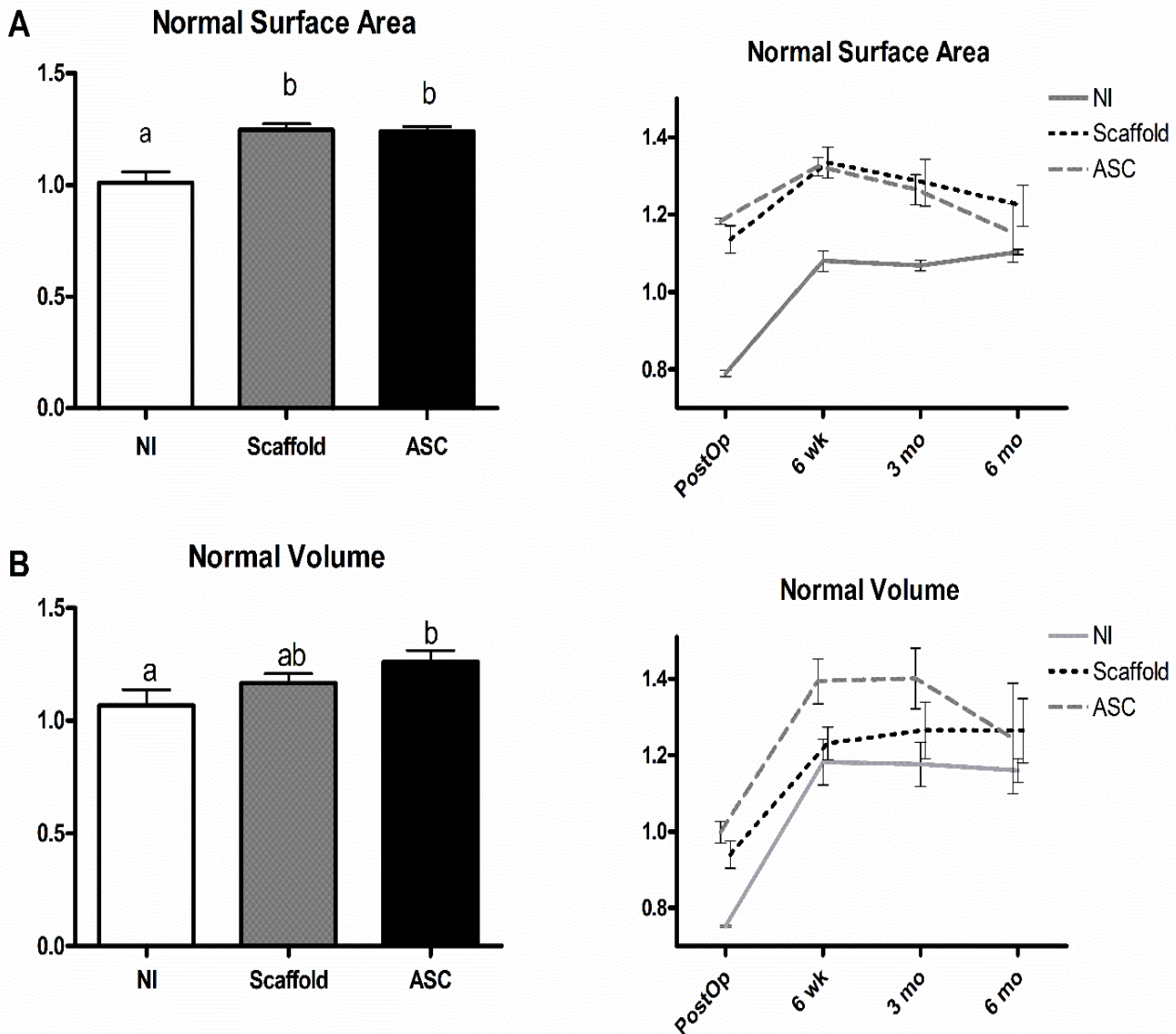


Figure 3.8: Significant differences by treatment in normalized bone surface area and volume. Bone surface area (SA) and volume was evaluated using computerized tomography scans at 4 time points. Measurements were normalized to preoperative baseline values. Significant differences are denoted by the letters “a” and “b” over the bar graphs. The bar graphs depict the mean values over the course of the study. The line graph shows the variation in SA and volume over time between treatments which had no significance. Statistical significance was set at $p \leq 0.05$ and error bars represent SEM.

3.4 Discussion

The immune modulating and osteogenic effects of ASCs are very well described through in vitro models and in vivo rodent models (2, 24, 30, 94, 107). The ability to evaluate the effect of ASC in vivo through blood values and noninvasive imaging is a tremendous advantage when it comes to clinical application. It can allow for better data collection and understanding of the use of ASCs in large animal models and in the clinical setting. The effects of treatment on systemic lymphocyte subpopulations and serum biomarkers of bone remodeling can be detected on a systemic level. The lower levels of systemic Th cell populations with the use of ASCs mimics results found in previous in vitro studies and on the local tissue level in vivo (16, 23, 29, 111) and contributes to acceptance of the first hypothesis. The hypothesis involving biomarkers and bone measurements could not be accepted as an increase in bone deposition could not be confirmed through CT images and biomarker values did not demonstrate a definitive picture of bone deposition. The results help to expand the available avenues for evaluating the use of ASCs in bone regeneration.

Regulation of the T cell response is a crucial part of graft acceptance. Autografts are the gold standard in bone grafts due in part to their lack of immune response. Unfortunately, lack of supply and donor site morbidity make this types of grafts impractical in large reconstructive surgeries. Allografts from cadavers are more common but come with complications of immune response and possible disease transmission. Engineered bone grafts using autologous ASCs and cancellous bone xenografts demonstrate the ability to replicate the biological benefits of the autograft with a possible limitless supply. The current study demonstrated a decrease in circulating Th cell population in ASC treated graft groups compared to empty grafts in an in vivo model. This is a novel approach for assessing the immune response to a local treatment with

ASCs. Most in vivo models assess the T cell response to MSCs by evaluating tissue samples post mortem through local tissue histopathology (35), immunohistochemistry, and PCR (107). The suppression of Th cell proliferation in the current study agrees with results of previous in vitro and in vivo studies (20, 25, 112). The mechanisms behind the immune modulatory effects of ASCs have been shown to include indoleamine 2,3-dioxygenase (IDO), prostaglandin E2, transforming growth factor-beta (TGF- β), interleukin-10 (IL-10), nitric oxide, and others. This wide range of elements gives support to the idea that ASCs can exploit different mechanisms in different situations. The effects of treatment on Th cell populations on the systemic level in this study help to validate this novel approach in assessing ASCs in tissue regeneration in vivo.

The use of systemic biomarkers for bone and cartilage metabolism to monitor clinical disease has been looked at extensively in human medicine (52, 53, 113). The major areas of focus are for osteoporosis, osteoarthritis, osteodystrophy, primary hyperparathyroidism, and neoplastic bone metastasis. It is very feasible that similar markers can be used to assess possible differences in osteogenesis between bone graft materials. The ability to correlate detectable changes in biomarkers with clinical alteration in bone metabolism has been best described in regard to neoplasia. Zhao et al. found that patients with bone metastasis had significantly higher levels of ICTP, procollagen type I N-terminal propeptide (PINP), BAP, and osteocalcin. These values could even be correlated to the number of bone metastasis sites (114). Similar findings were demonstrated in the current study in regards to ICTP being elevated in the ASC group. This is suggestive of an increase in bone resorption. This can result from either recipient bone resorption or remodeling of the xenograft. The lower levels of osteocalcin and BAP, in response to treatment with ASCs compared to the NI cohort, is indicative of decreased osteoblast activity. Decreases in osteoblast activity could result from decreased need for new bone formation (viable

graft) or an inhibition of osteoblast activation. The possibility of mature bone deposition with increased osteoclastogenesis and decreased osteoblastogenesis within the ASC cohort could also explain the differences seen. Though definitive interpretation of the treatment effect on biomarkers levels will require further studies, the ability to detect such effects is a step forward in their use in research.

The assessment of ASC contribution to bone remodeling through CT scanning is common practice in critical size defect models. The use of calvarian defects in rodents has been successful in demonstrating the benefits of MSCs in scaffold implants (36-38). Large animal models have also been used but generally evaluate a cylindrical defect in long bones (42, 74, 115). The current study was designed to look at replacing a large articulating defect which only has direct contact to supporting bone on 2 edges. This presents more possibilities for complications and fewer surfaces for osteoinduction and osteoconduction of the graft material. A treatment effect was demonstrated on measurements of SA and volume when all time points were considered together. The lower measurements of SA and volume in the NI group would suggest a decrease in bone formation. When the measurements of SA and volume are compared by treatment for the final time point alone (6 months) no differences are demonstrated. Figure 3.5 demonstrates the similarities in bone growth at the surgical site between treatments at each time point. The differences we were able to demonstrate during the study may have been confounded due to the presence of the cancellous graft material. Histopathology of the surgical sites was unavailable as they were used for a different study. Measurements of SA and volume from CT evaluation may lack sensitivity for the comparison of bone growth in the current model.

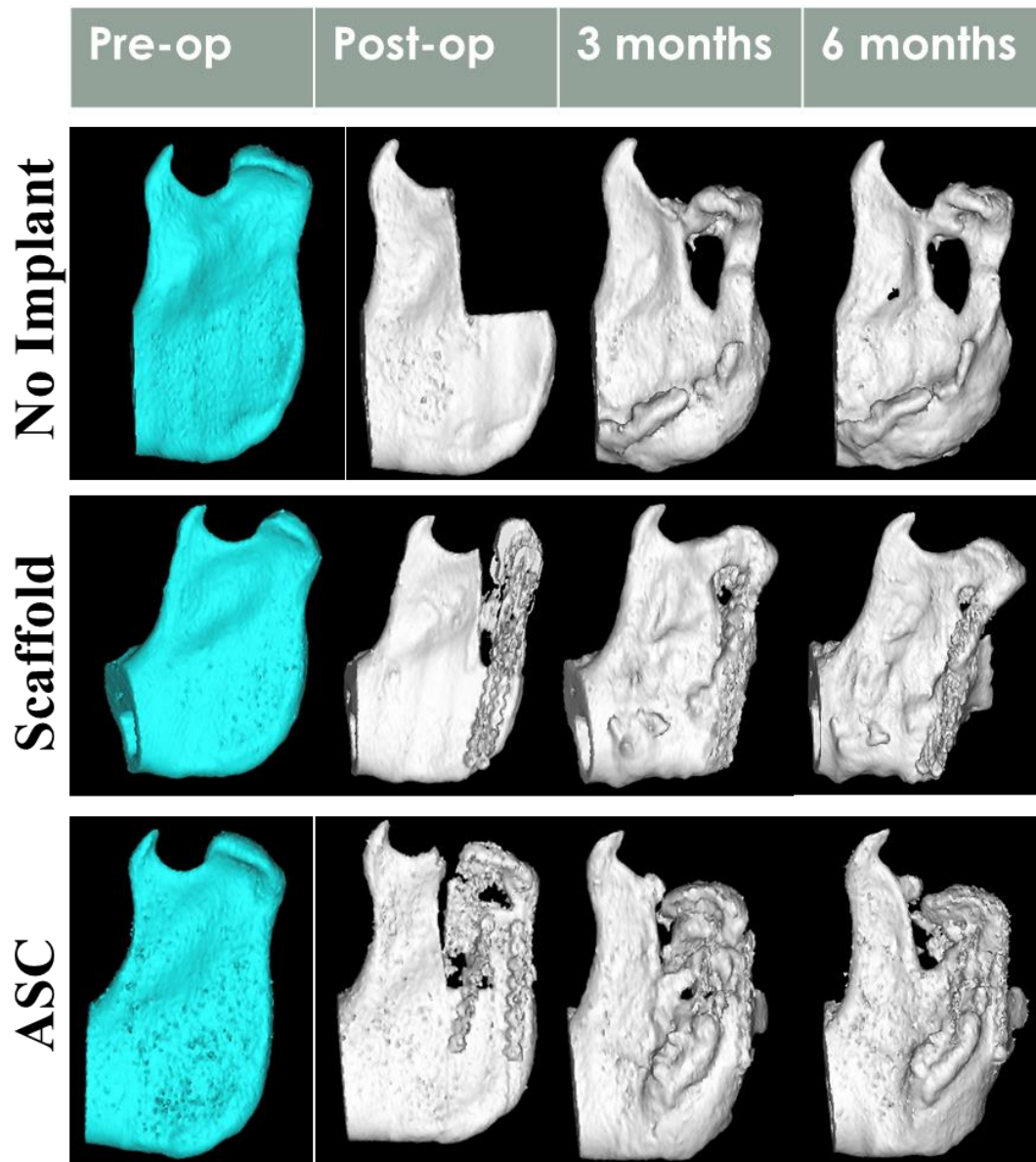


Figure 3.5: Computerized topography scans. Bone growth was evaluated throughout the study by computerized topography scans of the surgical area. The 3 dimensional reconstructed area was delineated cranially by the caudal aspect of the last molar and caudally by the caudal edge of the ramus. The images used above are representative samples from each treatment group. There were no differences between treatments in surface area or volume at the 6 month time point.

The present study demonstrates the ability to detect significant differences in circulating T cell populations and bone biomarkers in a swine model for bioengineered cancellous bone grafts. Lower population of systemic Th cells in the ASC group agrees with previous assessments of ASCs abilities to suppress the T cell response and help validate the ability to detect these effects on a systemic level. The effects on bone biomarkers evaluated in this study seem to indicate more bone resorption in the ASC and scaffold groups compared to the control. These findings were not supported by the CT evaluation of bone formation which showed no difference in SA or volume between groups at the final time point. Treatment effects were evident in the biomarker levels however interpretation of these effects requires further study. This study has given validation to the ability to assess ASC effects in bone remodeling from a systemic view point. Though further research is required in this area, the ability to detect treatment effect through hematologic parameters can open the door to novel techniques and models in the use of ASCs.

CHAPTER 4: DISCUSSION AND FUTURE RESEARCH

The study of ASCs in tissue engineering is an exciting and expanding field. The potential use of these cells for treatment of a wide variety of diseases and clinical problems is impressive. The findings in this paper help us to better understand the use of such technology in a large animal model and improve our understanding.

The inclusion of local nerve blocks in the veterinary medical field has expanded greatly in the last decade. This also includes the area of animal models in research. Regulatory requirements are focusing more on the wellbeing of the animals and avoidance of distress as our understanding of animal behavior improves. The assessment of pain is very difficult in animals and varies greatly amongst species. Our poor understanding of animal reactions to pain, within some species, make it difficult for us to properly address the issue. Our findings in this study helped to narrow the scope for pain assessment in pigs. Future studies in this area will be needed to pinpoint possible behaviors associated with pain in this model. Studies assessing different and possibly multiple nerve blocks are needed to add to the information presented here. The addition of mean alveolar concentration (MAC) measurements in future studies will aid in eliminating variation between subjects due to inhalant anesthesia. Though anatomically difficult for this particular study, the use of electromyography (EMG) to aid in confirming nerve blocks would greatly improve the viability of such studies.

The systemic evaluation of autologous ASC's effects on bone xenograft implants are feasible based on the data presented. Our findings may have raised more questions than answers but they also opened the door for new modalities of assessing the effects of ASCs. The results point to the ability of ASCs to prevent a Th cell response to the cancellous graft. Future studies may attempt to further describe cellular populations through additional CD markers. Additional CD

markers such as CD25 would help to address the idea that T_{reg} cells are up regulated. The ability to perform immunohistochemistry and histology on local lymph nodes and tissues in future studies would greatly expand their scientific contribution.

The results further verify the use of certain biomarker ELISAs in pigs for the assessment of orthopedic change which may help to elucidate the usefulness of these markers clinically.

Though the changes seen in the biomarkers were not correlated to the SA and volume measurements in this study, they may correlate better with a more precise method of evaluating bone growth. The use of nuclear scintigraphy or bone density could give more detailed information regarding bone remodeling. Placement of metallic markers such as bone screws or staples near the surgical sight could improve repeatability of such measurements and reduce variability.

Overall these studies identified new techniques to improve and expand the use of the swine facial reconstruction model. Our hope is that this will allow for a better understanding of the different avenues in which ASCs function to enhance regenerative medicine.

REFERENCES

1. Hoch AI, Leach JK. Concise review: optimizing expansion of bone marrow mesenchymal stem/stromal cells for clinical applications. *Stem cells translational medicine*. 2014 May;3(5):643-52. PubMed PMID: 24682286. Pubmed Central PMCID: 4006491. Epub 2014/04/01. eng.
2. Mizuno H, Tobita M, Uysal AC. Concise review: adipose-derived stem cells as a novel tool for future regenerative medicine. *Stem Cells*. 2012 May;30(5):804-10. PubMed PMID: 22415904. Epub 2012/03/15. eng.
3. Al-Nbaheen M, Vishnubalaji R, Ali D, Bouslimi A, Al-Jassir F, Megges M, et al. Human stromal (mesenchymal) stem cells from bone marrow, adipose tissue and skin exhibit differences in molecular phenotype and differentiation potential. *Stem cell reviews*. 2013 Feb;9(1):32-43. PubMed PMID: 22529014. Pubmed Central PMCID: 3563956. Epub 2012/04/25. eng.
4. Sassoon AA, Ozasa Y, Chikenji T, Sun YL, Larson DR, Maas ML, et al. Skeletal muscle and bone marrow derived stromal cells: a comparison of tenocyte differentiation capabilities. *Journal of orthopaedic research : official publication of the Orthopaedic Research Society*. 2012 Nov;30(11):1710-8. PubMed PMID: 22511232. Pubmed Central PMCID: 3402710. Epub 2012/04/19. eng.
5. Yoo KH, Jang IK, Lee MW, Kim HE, Yang MS, Eom Y, et al. Comparison of immunomodulatory properties of mesenchymal stem cells derived from adult human tissues. *Cellular immunology*. 2009;259(2):150-6. PubMed PMID: 19608159. Epub 2009/07/18. eng.
6. Pinnamaneni N, Funderburgh JL. Concise review: Stem cells in the corneal stroma. *Stem Cells*. 2012 Jun;30(6):1059-63. PubMed PMID: 22489057. Pubmed Central PMCID: 3580383. Epub 2012/04/11. eng.
7. Korbaling M, Estrov Z. Adult stem cells for tissue repair - a new therapeutic concept? *The New England journal of medicine*. 2003 Aug 7;349(6):570-82. PubMed PMID: 12904523. Epub 2003/08/09. eng.
8. Yoshimura K, Shigeura T, Matsumoto D, Sato T, Takaki Y, Aiba-Kojima E, et al. Characterization of freshly isolated and cultured cells derived from the fatty and fluid portions of liposuction aspirates. *Journal of cellular physiology*. 2006 Jul;208(1):64-76. PubMed PMID: 16557516. Epub 2006/03/25. eng.
9. Shi Y, Hu G, Su J, Li W, Chen Q, Shou P, et al. Mesenchymal stem cells: a new strategy for immunosuppression and tissue repair. *Cell research*. 2010 May;20(5):510-8. PubMed PMID: 20368733.
10. Dominici M, Le Blanc K, Mueller I, Slaper-Cortenbach I, Marini F, Krause D, et al. Minimal criteria for defining multipotent mesenchymal stromal cells. The International Society for Cellular Therapy position statement. *Cytotherapy*. 2006;8(4):315-7. PubMed PMID: 16923606. Epub 2006/08/23. eng.

11. Kokai LE, Marra K, Rubin JP. Adipose stem cells: biology and clinical applications for tissue repair and regeneration. *Translational research : the journal of laboratory and clinical medicine*. 2014 Apr;163(4):399-408. PubMed PMID: 24361334.
12. Murphy MB, Moncivais K, Caplan AI. Mesenchymal stem cells: environmentally responsive therapeutics for regenerative medicine. *Experimental & molecular medicine*. 2013;45:e54. PubMed PMID: 24232253. Pubmed Central PMCID: 3849579.
13. Fernandez Vallone VB, Romaniuk MA, Choi H, Labovsky V, Otaegui J, Chasseing NA. Mesenchymal stem cells and their use in therapy: what has been achieved? *Differentiation; research in biological diversity*. 2013 Jan;85(1-2):1-10. PubMed PMID: 23314286.
14. Locke M, Feisst V, Dunbar PR. Concise review: human adipose-derived stem cells: separating promise from clinical need. *Stem Cells*. 2011 Mar;29(3):404-11. PubMed PMID: 21425404.
15. Langenbach F, Handschel J. Effects of dexamethasone, ascorbic acid and beta-glycerophosphate on the osteogenic differentiation of stem cells in vitro. *Stem cell research & therapy*. 2013;4(5):117. PubMed PMID: 24073831. Pubmed Central PMCID: 3854789.
16. Yanez R, Lamana ML, Garcia-Castro J, Colmenero I, Ramirez M, Bueren JA. Adipose tissue-derived mesenchymal stem cells have in vivo immunosuppressive properties applicable for the control of the graft-versus-host disease. *Stem Cells*. 2006 Nov;24(11):2582-91. PubMed PMID: 16873762. Epub 2006/07/29. eng.
17. Fang B, Song Y, Liao L, Zhang Y, Zhao RC. Favorable response to human adipose tissue-derived mesenchymal stem cells in steroid-refractory acute graft-versus-host disease. *Transplantation proceedings*. 2007 Dec;39(10):3358-62. PubMed PMID: 18089385. Epub 2007/12/20. eng.
18. Fang B, Song Y, Zhao RC, Han Q, Lin Q. Using human adipose tissue-derived mesenchymal stem cells as salvage therapy for hepatic graft-versus-host disease resembling acute hepatitis. *Transplantation proceedings*. 2007 Jun;39(5):1710-3. PubMed PMID: 17580228. Epub 2007/06/21. eng.
19. Gonzalez MA, Gonzalez-Rey E, Rico L, Buscher D, Delgado M. Adipose-derived mesenchymal stem cells alleviate experimental colitis by inhibiting inflammatory and autoimmune responses. *Gastroenterology*. 2009 Mar;136(3):978-89. PubMed PMID: 19135996.
20. Gonzalez-Rey E, Gonzalez MA, Varela N, O'Valle F, Hernandez-Cortes P, Rico L, et al. Human adipose-derived mesenchymal stem cells reduce inflammatory and T cell responses and induce regulatory T cells in vitro in rheumatoid arthritis. *Annals of the rheumatic diseases*. 2010 Jan;69(1):241-8. PubMed PMID: 19124525. Epub 2009/01/07. eng.
21. Ra JC, Kang SK, Shin IS, Park HG, Joo SA, Kim JG, et al. Stem cell treatment for patients with autoimmune disease by systemic infusion of culture-expanded autologous adipose tissue derived mesenchymal stem cells. *Journal of translational medicine*. 2011;9:181. PubMed PMID: 22017805. Pubmed Central PMCID: 3222617.

22. Frazier TP, McLachlan JB, Gimble JM, Tucker HA, Rowan BG. Human adipose-derived stromal/stem cells induce functional CD4+CD25+FoxP3+CD127- regulatory T cells under low oxygen culture conditions. *Stem cells and development*. 2014 May 1;23(9):968-77. PubMed PMID: 24405386. Pubmed Central PMCID: 3997145. Epub 2014/01/11. eng.
23. Kim JH, Lee YT, Hong JM, Hwang YI. Suppression of in vitro murine T cell proliferation by human adipose tissue-derived mesenchymal stem cells is dependent mainly on cyclooxygenase-2 expression. *Anatomy & cell biology*. 2013 Dec;46(4):262-71. PubMed PMID: 24386599. Pubmed Central PMCID: 3875844. Epub 2014/01/05. eng.
24. Leto Barone AA, Khalifian S, Lee WP, Brandacher G. Immunomodulatory effects of adipose-derived stem cells: fact or fiction? *BioMed research international*. 2013;2013:383685. PubMed PMID: 24106704. Pubmed Central PMCID: 3782761.
25. Keyser KA, Beagles KE, Kiem HP. Comparison of mesenchymal stem cells from different tissues to suppress T-cell activation. *Cell transplantation*. 2007;16(5):555-62. PubMed PMID: 17708345. Epub 2007/08/22. eng.
26. Duffy MM, Ritter T, Ceredig R, Griffin MD. Mesenchymal stem cell effects on T-cell effector pathways. *Stem cell research & therapy*. 2011;2(4):34. PubMed PMID: 21861858. Pubmed Central PMCID: 3219065.
27. Cui L, Yin S, Liu W, Li N, Zhang W, Cao Y. Expanded adipose-derived stem cells suppress mixed lymphocyte reaction by secretion of prostaglandin E2. *Tissue engineering*. 2007 Jun;13(6):1185-95. PubMed PMID: 17518704. Epub 2007/05/24. eng.
28. DelaRosa O, Lombardo E, Beraza A, Mancheno-Corvo P, Ramirez C, Menta R, et al. Requirement of IFN-gamma-mediated indoleamine 2,3-dioxygenase expression in the modulation of lymphocyte proliferation by human adipose-derived stem cells. *Tissue engineering Part A*. 2009 Oct;15(10):2795-806. PubMed PMID: 19231921. Epub 2009/02/24. eng.
29. Quaedackers ME, Baan CC, Weimar W, Hoogduijn MJ. Cell contact interaction between adipose-derived stromal cells and allo-activated T lymphocytes. *European journal of immunology*. 2009 Dec;39(12):3436-46. PubMed PMID: 19798683. Epub 2009/10/03. eng.
30. Minteer D, Marra KG, Rubin JP. Adipose-derived mesenchymal stem cells: biology and potential applications. *Advances in biochemical engineering/biotechnology*. 2013;129:59-71. PubMed PMID: 22825719.
31. Clarke B. Normal bone anatomy and physiology. *Clinical journal of the American Society of Nephrology : CJASN*. 2008 Nov;3 Suppl 3:S131-9. PubMed PMID: 18988698. Pubmed Central PMCID: 3152283.
32. Nagae M, Hiraga T, Yoneda T. Acidic microenvironment created by osteoclasts causes bone pain associated with tumor colonization. *Journal of bone and mineral metabolism*. 2007;25(2):99-104. PubMed PMID: 17323179.

33. Centrella M, McCarthy TL, Canalis E. Transforming growth factor-beta and remodeling of bone. *The Journal of bone and joint surgery American volume*. 1991 Oct;73(9):1418-28. PubMed PMID: 1918129.
34. Anderson HC. Matrix vesicles and calcification. *Current rheumatology reports*. 2003 Jun;5(3):222-6. PubMed PMID: 12744815.
35. McIntosh KR, Lopez MJ, Borneman JN, Spencer ND, Anderson PA, Gimble JM. Immunogenicity of allogeneic adipose-derived stem cells in a rat spinal fusion model. *Tissue engineering Part A*. 2009 Sep;15(9):2677-86. PubMed PMID: 19207041. Pubmed Central PMCID: 2746330. Epub 2009/02/12. eng.
36. Choi JW, Park EJ, Shin HS, Shin IS, Ra JC, Koh KS. In vivo differentiation of undifferentiated human adipose tissue-derived mesenchymal stem cells in critical-sized calvarial bone defects. *Annals of plastic surgery*. 2014 Feb;72(2):225-33. PubMed PMID: 23221992. Epub 2012/12/12. eng.
37. Levi B, James AW, Nelson ER, Vistnes D, Wu B, Lee M, et al. Human adipose derived stromal cells heal critical size mouse calvarial defects. *PloS one*. 2010;5(6):e11177. PubMed PMID: 20567510. Pubmed Central PMCID: 2887361. Epub 2010/06/23. eng.
38. Cowan CM, Shi YY, Aalami OO, Chou YF, Mari C, Thomas R, et al. Adipose-derived adult stromal cells heal critical-size mouse calvarial defects. *Nature biotechnology*. 2004 May;22(5):560-7. PubMed PMID: 15077117. Epub 2004/04/13. eng.
39. Stephan SJ, Tholpady SS, Gross B, Petrie-Aronin CE, Botchway EA, Nair LS, et al. Injectable tissue-engineered bone repair of a rat calvarial defect. *The Laryngoscope*. 2010 May;120(5):895-901. PubMed PMID: 20422682. Pubmed Central PMCID: 3115737.
40. Ruehe B, Niehues S, Heberer S, Nelson K. Miniature pigs as an animal model for implant research: bone regeneration in critical-size defects. *Oral surgery, oral medicine, oral pathology, oral radiology, and endodontics*. 2009 Nov;108(5):699-706. PubMed PMID: 19782620.
41. Ren ML, Peng W, Yang ZL, Sun XJ, Zhang SC, Wang ZG, et al. Allogeneic adipose-derived stem cells with low immunogenicity constructing tissue-engineered bone for repairing bone defects in pigs. *Cell transplantation*. 2012;21(12):2711-21. PubMed PMID: 22963757.
42. Niemeyer P, Fechner K, Milz S, Richter W, Suedkamp NP, Mehlhorn AT, et al. Comparison of mesenchymal stem cells from bone marrow and adipose tissue for bone regeneration in a critical size defect of the sheep tibia and the influence of platelet-rich plasma. *Biomaterials*. 2010 May;31(13):3572-9. PubMed PMID: 20153047. Epub 2010/02/16. eng.
43. Burwell RG. Studies in the Transplantation of Bone. Vii. The Fresh Composite Homograft-Autograft of Cancellous Bone; an Analysis of Factors Leading to Osteogenesis in Marrow Transplants and in Marrow-Containing Bone Grafts. *The Journal of bone and joint surgery British volume*. 1964 Feb;46:110-40. PubMed PMID: 14126228. Epub 1964/02/01. eng.

44. Cypher TJ, Grossman JP. Biological principles of bone graft healing. *The Journal of foot and ankle surgery : official publication of the American College of Foot and Ankle Surgeons*. 1996 Sep-Oct;35(5):413-7. PubMed PMID: 8915864. Epub 1996/09/01. eng.
45. Cornell CN, Lane JM. Current understanding of osteoconduction in bone regeneration. *Clinical orthopaedics and related research*. 1998 Oct(355 Suppl):S267-73. PubMed PMID: 9917646. Epub 1999/01/26. eng.
46. Albrektsson T, Johansson C. Osteoinduction, osteoconduction and osseointegration. *European spine journal : official publication of the European Spine Society, the European Spinal Deformity Society, and the European Section of the Cervical Spine Research Society*. 2001 Oct;10 Suppl 2:S96-101. PubMed PMID: 11716023. Pubmed Central PMCID: 3611551. Epub 2001/11/22. eng.
47. Miron RJ, Zhang YF. Osteoinduction: a review of old concepts with new standards. *Journal of dental research*. 2012 Aug;91(8):736-44. PubMed PMID: 22318372. Epub 2012/02/10. eng.
48. Demers LM, Costa L, Lipton A. Biochemical markers and skeletal metastases. *Clinical orthopaedics and related research*. 2003 Oct(415 Suppl):S138-47. PubMed PMID: 14600604. Epub 2003/11/06. eng.
49. Fardellone P, Sejourne A, Paccou J, Goeb V. Bone Remodelling Markers in Rheumatoid Arthritis. *Mediators of inflammation*. 2014;2014:484280. PubMed PMID: 24839355. Epub 2014/05/20. Eng.
50. Tang C, Liu Y, Qin H, Li X, Guo W, Li J, et al. Clinical significance of serum BAP, TRACP 5b and ICTP as bone metabolic markers for bone metastasis screening in lung cancer patients. *Clinica chimica acta; international journal of clinical chemistry*. 2013 Nov 15;426:102-7. PubMed PMID: 24055775. Epub 2013/09/24. eng.
51. Frantz NZ, Friesen KG, Andrews GA, Tokach MD, Yamka RM, Loughin TL, et al. Use of serum biomarkers to predict the development and severity of osteochondrosis lesions in the distal portion of the femur in pigs. *American journal of veterinary research*. 2010 Aug;71(8):946-52. PubMed PMID: 20673095.
52. Garnero P. Biomarkers for osteoporosis management: utility in diagnosis, fracture risk prediction and therapy monitoring. *Molecular diagnosis & therapy*. 2008;12(3):157-70. PubMed PMID: 18510379. Epub 2008/05/31. eng.
53. Lotz M, Martel-Pelletier J, Christiansen C, Brandi ML, Bruyere O, Chapurlat R, et al. Value of biomarkers in osteoarthritis: current status and perspectives. *Annals of the rheumatic diseases*. 2013 Nov;72(11):1756-63. PubMed PMID: 23897772. Pubmed Central PMCID: 3812859.
54. Papadaki ME, Troulis MJ, Glowacki J, Kaban LB. A minipig model of maxillary distraction osteogenesis. *Journal of oral and maxillofacial surgery : official journal of the*

American Association of Oral and Maxillofacial Surgeons. 2010 Nov;68(11):2783-91. PubMed PMID: 20971370. Epub 2010/10/26. eng.

55. Herring SW, Decker JD, Liu ZJ, Ma T. Temporomandibular joint in miniature pigs: anatomy, cell replication, and relation to loading. *The Anatomical record*. 2002 Mar 1;266(3):152-66. PubMed PMID: 11870598.

56. Schlegel KA, Rupprecht S, Petrovic L, Honert C, Srour S, von Wilmowsky C, et al. Preclinical animal model for de novo bone formation in human maxillary sinus. *Oral surgery, oral medicine, oral pathology, oral radiology, and endodontics*. 2009 Sep;108(3):e37-44. PubMed PMID: 19716490.

57. Olopade JO, Okandeji ME. A study of some rostrfacial indices related to regional anaesthesia of the porcine: implications as an animal model for dental research. *Nigerian journal of physiological sciences : official publication of the Physiological Society of Nigeria*. 2010;25(2):159-64. PubMed PMID: 22314955. Epub 2010/01/01. eng.

58. Kanakaraj M, Shanmugasundaram N, Chandramohan M, Kannan R, Perumal SM, Nagendran J. Regional anesthesia in faciomaxillary and oral surgery. *Journal of pharmacy & bioallied sciences*. 2012 Aug;4(Suppl 2):S264-9. PubMed PMID: 23066267. Pubmed Central PMCID: 3467933.

59. Lizarraga I, Janovyak E, Beths T. Comparing lidocaine, bupivacaine and a lidocaine-bupivacaine mixture as a metacarpal block in sheep. *Vet J*. 2013 Feb 7. PubMed PMID: 23394846. Epub 2013/02/12. Eng.

60. Chahar P, Cummings KC, 3rd. Liposomal bupivacaine: a review of a new bupivacaine formulation. *Journal of pain research*. 2012;5:257-64. PubMed PMID: 23049275. Pubmed Central PMCID: 3442744.

61. Sasaki R, Watanabe Y, Yamato M, Aoki S, Okano T, Ando T. Surgical anatomy of the swine face. *Laboratory animals*. 2010 Oct;44(4):359-63. PubMed PMID: 20696789. Epub 2010/08/11. eng.

62. Trullenque-Eriksson A, Guisado-Moya B. Comparative study of two local anesthetics in the surgical extraction of mandibular third molars: bupivacaine and articaine. *Medicina oral, patologia oral y cirugia bucal*. 2011 May;16(3):e390-6. PubMed PMID: 21196829.

63. Carotenuto AM, Ravasio G, Fonda D, Stefanello D. Proximal mandibular nerve block, using electrolocation, for rostral mandibulectomy in a geriatric dog. *The Canadian veterinary journal La revue veterinaire canadienne*. 2011 May;52(5):515-8. PubMed PMID: 22043072. Pubmed Central PMCID: 3078005. Epub 2011/11/02. eng.

64. Mamiya H, Ichinohe T, Kaneko Y. Effects of block analgesia on attenuating intraoperative stress responses during oral surgery. *Anesthesia progress*. 1997 Summer;44(3):101-5. PubMed PMID: 9481970. Pubmed Central PMCID: 2148925.

65. Gouin JP, Kiecolt-Glaser JK. The impact of psychological stress on wound healing: methods and mechanisms. *Critical care nursing clinics of North America*. 2012 Jun;24(2):201-13. PubMed PMID: 22548859.
66. Walburn J, Vedhara K, Hankins M, Rixon L, Weinman J. Psychological stress and wound healing in humans: a systematic review and meta-analysis. *Journal of psychosomatic research*. 2009 Sep;67(3):253-71. PubMed PMID: 19686881.
67. Kronsteiner B, Wolbank S, Peterbauer A, Hackl C, Redl H, van Griensven M, et al. Human mesenchymal stem cells from adipose tissue and amnion influence T-cells depending on stimulation method and presence of other immune cells. *Stem cells and development*. 2011 Dec;20(12):2115-26. PubMed PMID: 21381973.
68. Holt TR, Withington DE, Mitchell E. Which pressure to believe? A comparison of direct arterial with indirect blood pressure measurement techniques in the pediatric intensive care unit. *Pediatric critical care medicine : a journal of the Society of Critical Care Medicine and the World Federation of Pediatric Intensive and Critical Care Societies*. 2011 Nov;12(6):e391-4. PubMed PMID: 21666539. Epub 2011/06/15. eng.
69. Lehman LW, Saeed M, Talmor D, Mark R, Malhotra A. Methods of blood pressure measurement in the ICU. *Critical care medicine*. 2013 Jan;41(1):34-40. PubMed PMID: 23269127. Epub 2012/12/28. eng.
70. Stover JF, Stocker R, Lenherr R, Neff TA, Cottini SR, Zoller B, et al. Noninvasive cardiac output and blood pressure monitoring cannot replace an invasive monitoring system in critically ill patients. *BMC anesthesiology*. 2009;9:6. PubMed PMID: 19821993. Pubmed Central PMCID: 2766368. Epub 2009/10/14. eng.
71. King JW, Bair E, Duggan D, Maixner W, Khan AA. The relationship between resting arterial blood pressure and acute postoperative pain in endodontic patients. *Journal of orofacial pain*. 2012 Fall;26(4):321-7. PubMed PMID: 23110272.
72. Sacco M, Meschi M, Regolisti G, Detrenis S, Bianchi L, Bertorelli M, et al. The relationship between blood pressure and pain. *Journal of clinical hypertension*. 2013 Aug;15(8):600-5. PubMed PMID: 23889724.
73. Abukawa H, Shin M, Williams WB, Vacanti JP, Kaban LB, Troulis MJ. Reconstruction of mandibular defects with autologous tissue-engineered bone. *Journal of oral and maxillofacial surgery : official journal of the American Association of Oral and Maxillofacial Surgeons*. 2004 May;62(5):601-6. PubMed PMID: 15122567. Epub 2004/05/04. eng.
74. Wilson SM, Goldwasser MS, Clark SG, Monaco E, Bionaz M, Hurley WL, et al. Adipose-derived mesenchymal stem cells enhance healing of mandibular defects in the ramus of swine. *Journal of oral and maxillofacial surgery : official journal of the American Association of Oral and Maxillofacial Surgeons*. 2012 Mar;70(3):e193-203. PubMed PMID: 22374062.

75. Pearce AI, Richards RG, Milz S, Schneider E, Pearce SG. Animal models for implant biomaterial research in bone: a review. *European cells & materials*. 2007;13:1-10. PubMed PMID: 17334975.
76. Van Lancker P, Abeloos JV, De Clercq CA, Mommaerts MY. The effect of mandibular nerve block on opioid consumption, nausea and vomiting in bilateral mandibular osteotomies. *Acta anaesthesiologica Belgica*. 2003;54(3):223-6. PubMed PMID: 14598619. Epub 2003/11/06. eng.
77. Plantevin F, Pascal J, Morel J, Roussier M, Charier D, Prades JM, et al. Effect of mandibular nerve block on postoperative analgesia in patients undergoing oropharyngeal carcinoma surgery under general anaesthesia. *British journal of anaesthesia*. 2007 Nov;99(5):708-12. PubMed PMID: 17884802. Epub 2007/09/22. eng.
78. Splinter WM, Thomson ME. Somatic paravertebral block decreases opioid requirements in children undergoing appendectomy. *Canadian journal of anaesthesia = Journal canadien d'anesthesie*. 2010 Mar;57(3):206-10. PubMed PMID: 20063137. Epub 2010/01/12. eng.
79. Teofilo JM, Giovanini GS, Fracon RN, Lamano T. Histometric study of alveolar bone healing in rats treated with the nonsteroidal anti-inflammatory drug nimesulide. *Implant dentistry*. 2011 Apr;20(2):e7-13. PubMed PMID: 21448017. Epub 2011/03/31. eng.
80. Pountos I, Giannoudis PV, Jones E, English A, Churchman S, Field S, et al. NSAIDS inhibit in vitro MSC chondrogenesis but not osteogenesis: implications for mechanism of bone formation inhibition in man. *Journal of cellular and molecular medicine*. 2011 Mar;15(3):525-34. PubMed PMID: 20070439. Epub 2010/01/15. eng.
81. Welting TJ, Caron MM, Emans PJ, Janssen MP, Sanen K, Coolsen MM, et al. Inhibition of cyclooxygenase-2 impacts chondrocyte hypertrophic differentiation during endochondral ossification. *European cells & materials*. 2011;22:420-36; discussion 36-7. PubMed PMID: 22183916. Epub 2011/12/21. eng.
82. Yoon DS, Yoo JH, Kim YH, Paik S, Han CD, Lee JW. The effects of COX-2 inhibitor during osteogenic differentiation of bone marrow-derived human mesenchymal stem cells. *Stem cells and development*. 2010 Oct;19(10):1523-33. PubMed PMID: 20095820. Epub 2010/01/26. eng.
83. Kim HS, Lee HK, Jeong HS, Shin HW. Decreased postoperative pain after reduction of fractured nasal bones using a nerve block of the anterior ethmoidal nerve. *International journal of oral and maxillofacial surgery*. 2013 Mar 23. PubMed PMID: 23528745. Epub 2013/03/27. Eng.
84. Boonsiriseth K, Sirintawat N, Arunakul K, Wongsirichat N. Comparative study of the novel and conventional injection approach for inferior alveolar nerve block. *International journal of oral and maxillofacial surgery*. 2012 Dec 18. PubMed PMID: 23265758. Epub 2012/12/26. Eng.

85. Ogle OE, Mahjoubi G. Local anesthesia: agents, techniques, and complications. *Dental clinics of North America*. 2012 Jan;56(1):133-48, ix. PubMed PMID: 22117947. Epub 2011/11/29. eng.
86. Dyhre H, Lang M, Wallin R, Renck H. The duration of action of bupivacaine, levobupivacaine, ropivacaine and pethidine in peripheral nerve block in the rat. *Acta anaesthesiologica Scandinavica*. 1997 Nov;41(10):1346-52. PubMed PMID: 9422304. Epub 1998/01/09. eng.
87. Sawhney C, Agrawal P, Soni KD. Post operative pain relief through intermittent mandibular nerve block. *National journal of maxillofacial surgery*. 2011 Jan;2(1):80-1. PubMed PMID: 22442616. Pubmed Central PMCID: 3304218.
88. Singh B, Bhardwaj V. Continuous mandibular nerve block for pain relief. A report of two cases. *Canadian journal of anaesthesia = Journal canadien d'anesthesie*. 2002 Nov;49(9):951-3. PubMed PMID: 12419723. Epub 2002/11/07. eng.
89. Berde CB, Athiraman U, Yahalom B, Zurakowski D, Corfas G, Bogner C. Tetrodotoxin-bupivacaine-epinephrine combinations for prolonged local anesthesia. *Marine drugs*. 2011 Dec;9(12):2717-28. PubMed PMID: 22363247. Pubmed Central PMCID: 3280572. Epub 2012/03/01. eng.
90. Fanelli G, Casati A, Beccaria P, Aldegheri G, Berti M, Tarantino F, et al. A double-blind comparison of ropivacaine, bupivacaine, and mepivacaine during sciatic and femoral nerve blockade. *Anesthesia and analgesia*. 1998 Sep;87(3):597-600. PubMed PMID: 9728836. Epub 1998/09/05. eng.
91. Sinnott CJ, Cogswell LP, Johnson A, Strichartz GR. On the mechanism by which epinephrine potentiates lidocaine's peripheral nerve block. *Anesthesiology*. 2003 Jan;98(1):181-8. PubMed PMID: ISI:000180207300026. English.
92. Marra KG, Rubin JP. The potential of adipose-derived stem cells in craniofacial repair and regeneration. *Birth defects research Part C, Embryo today : reviews*. 2012 Mar;96(1):95-7. PubMed PMID: 22457180. Epub 2012/03/30. eng.
93. Gonzalez MA, Bernad A. Characteristics of adult stem cells. *Advances in experimental medicine and biology*. 2012;741:103-20. PubMed PMID: 22457106. Epub 2012/03/30. eng.
94. Knight MN, Hankenson KD. Mesenchymal Stem Cells in Bone Regeneration. *Advances in wound care*. 2013 Jul;2(6):306-16. PubMed PMID: 24527352. Pubmed Central PMCID: 3842877. Epub 2014/02/15. Eng.
95. Vidal MA, Kilroy GE, Lopez MJ, Johnson JR, Moore RM, Gimble JM. Characterization of equine adipose tissue-derived stromal cells: adipogenic and osteogenic capacity and comparison with bone marrow-derived mesenchymal stromal cells. *Veterinary surgery : VS*. 2007 Oct;36(7):613-22. PubMed PMID: 17894587.

96. Harris CT, Cooper LF. Comparison of bone graft matrices for human mesenchymal stem cell-directed osteogenesis. *Journal of biomedical materials research Part A*. 2004 Mar 15;68(4):747-55. PubMed PMID: 14986329. Epub 2004/02/27. eng.
97. Grayson WL, Frohlich M, Yeager K, Bhumiratana S, Chan ME, Cannizzaro C, et al. Engineering anatomically shaped human bone grafts. *Proceedings of the National Academy of Sciences of the United States of America*. 2010 Feb 23;107(8):3299-304. PubMed PMID: 19820164. Pubmed Central PMCID: 2840502.
98. Long B, Dan L, Jian L, Yunyu H, Shu H, Zhi Y. Evaluation of a novel reconstituted bone xenograft using processed bovine cancellous bone in combination with purified bovine bone morphogenetic protein. *Xenotransplantation*. 2012 Mar;19(2):122-32. PubMed PMID: 22497514. Epub 2012/04/14. eng.
99. Brocher J, Janicki P, Voltz P, Seebach E, Neumann E, Mueller-Ladner U, et al. Inferior ectopic bone formation of mesenchymal stromal cells from adipose tissue compared to bone marrow: rescue by chondrogenic pre-induction. *Stem cell research*. 2013 Nov;11(3):1393-406. PubMed PMID: 24140198.
100. Ma J, Both SK, Yang F, Cui FZ, Pan J, Meijer GJ, et al. Concise review: cell-based strategies in bone tissue engineering and regenerative medicine. *Stem cells translational medicine*. 2014 Jan;3(1):98-107. PubMed PMID: 24300556. Pubmed Central PMCID: 3902295.
101. Garnero P, Piperno M, Gineyts E, Christgau S, Delmas PD, Vignon E. Cross sectional evaluation of biochemical markers of bone, cartilage, and synovial tissue metabolism in patients with knee osteoarthritis: relations with disease activity and joint damage. *Annals of the rheumatic diseases*. 2001 Jun;60(6):619-26. PubMed PMID: 11350852. Pubmed Central PMCID: 1753666.
102. Issa F, Robb RJ, Wood KJ. The where and when of T cell regulation in transplantation. *Trends in immunology*. 2013 Mar;34(3):107-13. PubMed PMID: 23228885.
103. Scalea J, Hanecamp I, Robson SC, Yamada K. T-cell-mediated immunological barriers to xenotransplantation. *Xenotransplantation*. 2012 Jan;19(1):23-30. PubMed PMID: 22360750. Epub 2012/03/01. eng.
104. De Miguel MP, Fuentes-Julian S, Blazquez-Martinez A, Pascual CY, Aller MA, Arias J, et al. Immunosuppressive properties of mesenchymal stem cells: advances and applications. *Current molecular medicine*. 2012 Apr 18. PubMed PMID: 22515979. Epub 2012/04/21. Eng.
105. Cho KS, Roh HJ. Immunomodulatory effects of adipose-derived stem cells in airway allergic diseases. *Current stem cell research & therapy*. 2010 Jun;5(2):111-5. PubMed PMID: 19941459.
106. Larocca RA, Moraes-Vieira PM, Bassi EJ, Semedo P, de Almeida DC, da Silva MB, et al. Adipose tissue-derived mesenchymal stem cells increase skin allograft survival and inhibit Th-17 immune response. *PloS one*. 2013;8(10):e76396. PubMed PMID: 24124557. Pubmed Central PMCID: 3790669.

107. Roemeling-van Rhijn M, Khairoun M, Korevaar SS, Lievers E, Leuning DG, Ijzermans JN, et al. Human Bone Marrow- and Adipose Tissue-derived Mesenchymal Stromal Cells are Immunosuppressive and in a Humanized Allograft Rejection Model. *Journal of stem cell research & therapy*. 2013 Nov 25;Suppl 6(1):20780. PubMed PMID: 24672744. Pubmed Central PMCID: 3963708.
108. Fang B, Song Y, Lin Q, Zhang Y, Cao Y, Zhao RC, et al. Human adipose tissue-derived mesenchymal stromal cells as salvage therapy for treatment of severe refractory acute graft-vs.-host disease in two children. *Pediatric transplantation*. 2007 Nov;11(7):814-7. PubMed PMID: 17910665. Epub 2007/10/04. eng.
109. Williams KJ, Picou AA, Kish SL, Giraldo AM, Godke RA, Bondioli KR. Isolation and characterization of porcine adipose tissue-derived adult stem cells. *Cells, tissues, organs*. 2008;188(3):251-8. PubMed PMID: 18349524.
110. Weinberg A. PACTG PMBC Processing, Cryopreservation and Thawing Method. 2003 May 29, 2003:6.
111. Najar M, Raicevic G, Boufker HI, Fayyad-Kazan H, De Bruyn C, Meuleman N, et al. Adipose-tissue-derived and Wharton's jelly-derived mesenchymal stromal cells suppress lymphocyte responses by secreting leukemia inhibitory factor. *Tissue engineering Part A*. 2010 Nov;16(11):3537-46. PubMed PMID: 20597819. Epub 2010/07/06. eng.
112. Zappia E, Casazza S, Pedemonte E, Benvenuto F, Bonanni I, Gerdoni E, et al. Mesenchymal stem cells ameliorate experimental autoimmune encephalomyelitis inducing T-cell anergy. *Blood*. 2005 Sep 1;106(5):1755-61. PubMed PMID: 15905186. Epub 2005/05/21. eng.
113. Eastell R, Hannon RA. Biomarkers of bone health and osteoporosis risk. *The Proceedings of the Nutrition Society*. 2008 May;67(2):157-62. PubMed PMID: 18412989. Epub 2008/04/17. eng.
114. Zhao H, Han KL, Wang ZY, Chen Y, Li HT, Zeng JL, et al. Value of C-telopeptide-cross-linked Type I collagen, osteocalcin, bone-specific alkaline phosphatase and procollagen Type I N-terminal propeptide in the diagnosis and prognosis of bone metastasis in patients with malignant tumors. *Medical science monitor : international medical journal of experimental and clinical research*. 2011 Nov;17(11):CR626-33. PubMed PMID: 22037741. Pubmed Central PMCID: 3539492. Epub 2011/11/01. eng.
115. Schubert T, Lafont S, Beaurin G, Grisay G, Behets C, Gianello P, et al. Critical size bone defect reconstruction by an autologous 3D osteogenic-like tissue derived from differentiated adipose MSCs. *Biomaterials*. 2013 Jun;34(18):4428-38. PubMed PMID: 23507085.

APPENDIX

Materials required — not supplied

- Containers for preparing the Antibody Solution and the Washing Solution.
- Precision micropipettes to deliver 20 µL
- Distilled water
- Precision 8- or 12-channel multipipette to deliver 100 µL and 150 µL.
- Microtiter plate reader with both 450 nm and 650 nm filters

ASSAY PROCEDURE

For optimal performance of the assay it is important to comply with the instructions given below

Assay Procedure

Prior to use, prepare and equilibrate all solutions to room temperature. **Perform the assay at 18-22°C.**

Determine the number of strips needed for the assay. It is recommended to test all samples in duplicate. In addition, for each run a total of 16 wells are needed for the standards and controls. Place the appropriate number of strips in the plastic frame. Store unused immunostrips in the tightly closed foil bag with desiccant capsules.

1 Preparation of the Antibody Solution:

The **Antibody Solution** is prepared by 1) adding 10 mL of **Conjugate Diluent Solution** [BUF] to both the **Peroxidase Conjugated Antibody Solution** [ENZYMCNJ] and the **Biotinylated Antibody Solution** [Ab BIOTIN], and 2) mixing the two conjugate solutions in equal volumes.

2 Incubation in Immuno Strips

Pipette 20 µL of either **Standards** [CAL 0-5], **Controls** [CTRL 1-2], or unknown samples into appropriate wells followed by 150 µL of the **Antibody Solution**. Cover the immunostrips with sealing tape and incubate for 120±5 minutes at 18-22°C (without any mixing).

3 Washing

Wash the immunostrips 5 times manually with diluted **Washing Buffer** ([WASHBUF 50x] diluted 1+50 in distilled water). Using an automated plate washer, follow the instructions of the manufacturer or the guidelines of the laboratory. Usually 5 washing cycles are adequate. Make sure that the wells are **completely emptied** after each manual or automatic washing cycle.

4 Incubation with chromogenic substrate solution

Pipette 100 µL of the **Substrate Solution** [SUBS TMB] into each well and incubate for 15±2 minutes at 18-22°C in the dark (without any mixing). Use sealing tape. Do not pipette directly from the vial containing TMB substrate but transfer the needed volume to a clean reservoir. Remaining substrate in the reservoir should be discarded and not returned to vial TMB.

5 Stopping of colour reaction

Pipette 100 µL of the **Stopping Solution** [H2SO4] into each well.

6 Measurement of absorbance

Measure the absorbance at 450 nm with 650 nm as reference within two hours.

Limitations of the procedure

If the absorbance of a sample exceeds that of **Standard 5**, the sample should be diluted in **Standard 0** and re-analysed.

QUALITY CONTROL

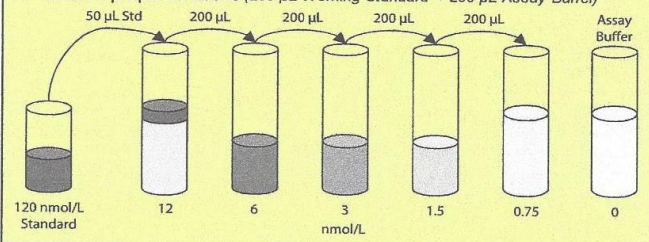
Good Laboratory Practice (GLP) requires the use of quality control specimens in each series of assays in order to check the performance of the assay. Controls should be treated as unknown samples, and the results analysed with appropriate statistical methods.

Additional File 1: Manufacturer's instructions for N-MID Osteocalcin ELISA kit

MicroVue™ Serum PYD EIA Summary

Reagent and Sample Preparation

- Dilute Controls 1:10 with Assay Buffer (50 µL Control + 450 µL Assay Buffer)
- Prepare 12 nmol/L Standard Solution by diluting the 120 nmol/L PYD Standard 1:10 with Assay Buffer (50 µL PYD Standard + 450 µL Assay Buffer)
- Produce 1:2 dilution series (depicted below) using the 12 nmol/L Standard Solution prepared above (200 µL Working Standard + 200 µL Assay Buffer)



Add ~ 200 µL of each serum sample to 30k MWCO Spinfilter

Centrifuge ~ 30 minutes at 3,000xg to 10,000xg

Assay Procedure

Pipette 50 µL Reagent 1 into assay wells using multichannel pipette

Pipette 25 µL **diluted** Standards, **diluted** Controls, and **undiluted** filtered Samples into assay wells

Pipette 75 µL **cold** Pyridinoline antibody into assay wells with sufficient force to ensure adequate mixing.

Cover plate and incubate **18–24 hours** at 2–8°C in the dark

- Prepare 1X Wash Buffer (Dilute 10X Wash Buffer 1:10 with deionized water)
- Prepare Enzyme Conjugate with 1X Wash Buffer, store at 20–28°C (Add 10 mL 1X Wash Buffer per vial of Conjugate)

Add 150 µL Enzyme Conjugate into assay wells

Incubate **60 ± 5 minutes** at 20–28°C

- Prepare Substrate Solution (30 – 60 min before use) Add one Substrate tablet per bottle of Substrate Buffer (Shake vigorously)

Pipette 150 µL Working Substrate Solution

Incubate **40 ± 5 min** at 20–28°C

Pipette 100 µL Stop Solution

Read the Optical Density at 405 nm.
Analyze the assay results using a 4-parameter curve fit
 $y = (A-D)/(1 + (x/C)^B) + D$

0607G (2009/06)

i

Additional File 2: Manufacturer's instructions for the MicroVue Serum PYD EIA kit

REAGENT PREPARATION

Bring reagents and materials for the assay to 20–28°C before use. After removing the needed reagents and materials, return unused items to 2–8°C.

Coated Strips

Remove Stripwell Frame and the required number of Coated Strips from the pouch (See table in ASSAY PROCEDURE Section). Ensure that the pouch containing any unused strips is completely resealed.

Wash Buffer

Prepare required amount of 1X Wash Buffer (see table) by diluting 10X Wash Buffer concentrate 1:10 with deionized water. Store at 20–28°C. Use 1X Wash Buffer within 21 days of preparation.

Working Substrate Solution

Prepare Working Substrate Solution within 1 hour of use. Put one Substrate Tablet into each required bottle of 20–28°C Substrate Buffer (see table). Allow 30–60 minutes for tablet(s) to dissolve. Vigorously shake bottle(s) to completely mix. Discard remaining Working Substrate Solution after use.

STORAGE

Store kit at 2–8°C. Do not freeze. Store unused reagents at 2–8°C. Equilibrate reagents to 20–28°C before use. Store 1X Wash Buffer (10X diluted) at 20–28°C.

SPECIMEN COLLECTION AND STORAGE

Collect serum using standard venipuncture technique. Specimens should be collected without anticoagulants and in such a way to avoid hemolysis. Allow the blood to clot and separate the serum by centrifugation. Serum can be stored for 5 days at 2–8°C, at ≤ –40°C for 12 months, or at ≤ –80°C for 36 months. Do not subject samples to more than 3 freeze/thaw cycles.

“Off the clot” serum, serum separator tube serum, Na heparin plasma, and Li heparin plasma yield substantially equivalent results. It is recommended that plasma samples not be prepared using chelating agents such as EDTA or citrate.

ASSAY PROCEDURE

Read entire product insert before beginning the assay.

See REAGENT PREPARATION before proceeding.

Determine amount of each reagent required for the number of strips to be used.

# of Strips	4	6	8	12
# of Samples (tested in duplicate)	8	16	24	40
Substrate (bottle)	1	1	2*	2*
1X Wash Buffer (mL)	100	150	200	300

*When more than one bottle or vial is to be used, combine the contents and mix prior to use.

Sample Incubation

1. Remove Stripwell Frame and the required number of Coated Strips from the pouch (see table) just prior to use. Ensure that the foil pouch containing any unused strips is completely resealed.

2. Place desired number of Coated Strips in the Stripwell Frame. Label strips to prevent mix-up in case of accidental removal from Stripwell Frame.
3. Add 125 µL Assay Buffer to each well.
4. Add 20 µL of Standards, Controls, and Specimens to assay wells. **Do not** mix with Assay Buffer by repeat pipetting. This step should be completed within 30 minutes. **Gently swirl plate to ensure mixing of sample and buffer.**
5. Incubate for 3 hours (± 10 minutes) at 20–28°C.
6. Prepare Working Substrate Solution within 1 hour of use. Put one Substrate Tablet into each required bottle of 20–28°C Substrate Buffer (see table). Allow 30–60 minutes for tablet(s) to dissolve. Vigorously shake bottle(s) to completely mix.

Washing Step

7. Prepare required amount of 1X Wash Buffer (see table) by diluting 10X Wash Buffer 1:10 with deionized water. Store at 20–28°C. Use 1X Wash Buffer within 21 days of preparation.
8. Manually invert/empty strips. Add at least 250 µL of 1X Wash Buffer to each well and manually invert/empty strips. Repeat three more times for a total of four washes. Vigorously blot the strips dry on paper towels after the last wash.

Substrate Incubation

9. Add 150 µL of Working Substrate Solution to each well. Discard remaining Working Substrate Solution after use.
10. Incubate for 30 minutes (± 5 minutes) at 20–28°C.

Stop/Read

11. Add 100 µL of Stop Solution to each well. Add Stop Solution in the same pattern and time intervals as the Substrate Solution addition.
12. Read the optical density at 405 nm. Assure that no large bubbles are present in the wells and that the bottoms of the strips are clean. Strips should be read within **15 minutes** of Stop Solution addition.
13. Quantitation software with a quadratic calibration curve fitting equation **must** be used to analyze the MicroVue BAP assay results.
Equation: $y = A + Bx + Cx^2$

QUALITY CONTROL

The Certificate of Analysis included in this kit is lot specific and is to be used to verify that the results obtained by your laboratory are similar to those obtained at Quidel. The optical density values are provided and are to be used as a guideline only. The results obtained by your laboratory may differ.

Quality control ranges are provided. The control values are intended to verify the validity of the curve and sample results. Each laboratory should establish its own parameters for acceptable assay limits. If the control values are NOT within your laboratory's acceptance limits, the assay results should be considered questionable and the samples should be repeated.

If the optical density of the MicroVue BAP Standard F is less than 1.0, the results should be considered questionable and the samples should be repeated.

PROCEDURE

Materials required but not provided

PIPETTES (50 µL, 100 µL, 500 µL), MICROTITRE PLATE SHAKER, MICROTITRE STRIP WASHER, PHOTOMETRIC PLATE READER, ABSORBENT PAPER, DISTILLED WATER

Reconstitution of reagents

Calibrators and Controls. Allow the vials to reach equilibrium at room temperature (18...25 °C) before opening. **Reconstitute** by adding 500 µL of distilled water to all vials. Cap and mix well by gentle swirling or inversion to avoid foaming. Allow to stand for 30 minutes before use.

Wash concentrate. Dilute the wash concentrate to 1000 mL (80 mL + 920 mL) with distilled water.

Details of the procedure

1. **Bring** all reagents, controls and patient samples to room temperature (18...25 °C) at least 30 minutes before use.
2. **Remove** excess strips from the plate frame, **return** them to the pouch and close tightly.
3. **Pipette** 50 µL of calibrator, control and patient sample in duplicate into appropriate microtitre wells. Reserve two wells for the substrate blank.
4. **Pipette** 50 µL of ICTP enzyme conjugate (red) into all wells except blanks.
5. **Pipette** 50 µL of ICTP antiserum (blue) into all wells except blanks. The antiserum must be applied to all wells within 3 minutes. The use of an electronic dispenser or multichannel pipette is recommended.
6. **Incubate** on a plate shaker at 18...25°C for 2 hours. Use a shaking **speed** of **600-1000 rpm**.
7. **Wash** the strips 4 times with the wash solution on a plate washer. Use an appropriate volume of the wash solution (300-500 µL/well is recommended) and program for flat-bottom plates. Remove any remaining moisture by tapping the strips firmly against absorbent paper. Press the long sides of the holder firmly, so that the strips do not drop off. **Note: Proper washing is crucial for the assay performance.**
8. **Pipette** 100 µL of ICTP substrate into all wells.
9. **Incubate** on a plate shaker at 18...25 °C for 30 minutes.
10. **Stop** the enzyme reaction by adding 100 µL of stopping solution into all wells. **Shake** for 15-30 seconds to mix the reagents.
11. **Read** the absorbances of all wells at 450 nm on a plate reader within 10 minutes.

Additional File 4: Manufacturer's instructions for the UniQ ICTP EIA kit

2. PROTOCOL

Bring CP II ELISA kit to room temperature before use (20-25°C). Wear gloves for all steps of the protocol.

Note 1: Gently centrifuge small tubes before opening to ensure proper recovery of reagents.

Note 2: Reagents and samples must be gently vortexed just before use.

- Make standards according to Table 1.
- Add 50 µL of CP II standards and samples to the polypropylene mixing plate. Serum samples should be diluted 1/2 with Buffer III. This can be done directly on the plate (25 µL serum + 25 µL Buffer III). *Note: CP II binds to glass, make up CP II Std. in polypropylene tubes.*
- Add 50 µL of CP II Antibody diluted in Assay Buffer to all wells of the polypropylene mixing plate. (One Plate: 50 µL of CP II Antibody + 6 mL Assay Buffer).
- Pre-incubate the polypropylene mixing plate on a high speed Titre Plate Shaker at 600-700 rpm, covered, for 60 minutes (± 2 minutes) at room temperature (20-25°C).
- Remove the CP II ELISA plate from the foil pouch. Transfer 80 µL of antigen-antibody mixture from each well of the polypropylene mixing plate to the corresponding well of the ELISA plate using a multi-channel pipette.
- Incubate the covered ELISA plate on a high speed Titre Plate Shaker at 600-700 rpm for 2 hours (± 8 minutes) at room temperature (20-25°C).
- Wash the ELISA plate 6 times. Blot the plate dry on towels after the last wash.
- Add 100 µL/well of GAR-HRP conjugate diluted in Buffer III. (One Plate: 50 µL of GAR-HRP / 11 mL Buffer III).
- Incubate the covered ELISA plate on high speed Titre Plate Shaker at 600-700 rpm for 30 minutes (± 2 minutes) at room temperature (20-25°C).
- Wash the ELISA plate 6 times. Blot the plate dry on towels after the last wash.
- Add 100 µL of TMB/well.
- Incubate the covered ELISA plate on a high speed Titre Plate Shaker at 600-700 rpm for approximately 30 minutes at room temperature (20-25°C). Monitor colour development at 630 nm if necessary.
- Stop reaction by adding 100 µL of Stop Solution/well.
- Read plate at 450 nm within 10 minutes.

Additional File 5: Manufacturer's instructions for the CPII ELISA kit

2. PROTOCOL

Bring CS846 ELISA kit to room temperature before use. Wear gloves for all steps of the protocol.

Note: Centrifuge small tubes before opening to ensure proper recovery of reagents.

- Make standards according to Table 1.
- Remove the CS846 ELISA plate from the foil pouch.
- Add 50 µL / well of CS846 Standards and Samples to appropriate wells of the ELISA plate. Serum samples should be diluted 1:5 with Buffer III. This can be done directly on the plate (10 µL serum + 40 µL Buffer III).
- Add 50 µL of CS846-Biotin diluted in Assay Buffer to all wells of the ELISA plate (one Plate: 50 µL of stock + 6 ml of Assay Buffer).
- Add 50 µL / well of CS846 Antibody diluted in Assay Buffer to all wells of the ELISA plate (one Plate: 50 µL of stock + 6 ml of Assay buffer).
- Incubate the ELISA plate on high speed titre plate shaker at 600-700 rpm for 2 hours (± 8 minutes) at room temperature (20-25°C).
- Wash the ELISA plate 6 times. Vigorously blot the plate dry on towels after the last wash.
- Add 100 µL / well of Streptavidin-HRP conjugate diluted in Buffer III. (One Plate: 50 µL of stock + 11 mL Buffer III).
- Incubate the ELISA plate on high speed titre plate shaker at 600-700 rpm for 30 minutes (± 2 minutes) at room temperature (20-25°C).
- Wash plate 6 times. Vigorously blot the plate dry on towels after the last wash.
- Add 100 µL/ well of TMB. Warm aliquot of TMB to room temperature (20-25°C) in advance.
- Incubate on high speed titre plate shaker at 600-700 rpm for approximately 30 minutes at room temperature. Monitor colour development at 630 nm if necessary.
- Stop reaction by adding 100 µL of Stop Solution / well.
- Read plate at 450 nm within 10 min.

Additional File 6: Manufacturer's instructions for the CS 846 ELISA kit

VITA

Jonathan was born in Lancaster Pennsylvania in 1983. He received bachelor degrees in both Animal Science and International Finance at the University of Arkansas at Fayetteville in 2006 and 2008 respectively. Jonathan came to Louisiana State University for the veterinary medicine program and received his Doctorate in Veterinary Medicine in 2011. He continued his training in a residency program for Laboratory Animal medicine at LSU while simultaneously studying to attain his Masters degree.